International Telecommunication Union

ITU-R
Radiocommunication Sector of ITU

Report ITU-R BT.2382-0
(07/2015)

Description of interference into a digital terrestrial television receiver

BT Series

Broadcasting service
(television)

Foreword

The role of the Radiocommunication Sector is to ensure the rational, equitable, efficient and economical use of the radio-frequency spectrum by all radiocommunication services, including satellite services, and carry out studies without limit of frequency range on the basis of which Recommendations are adopted.

The regulatory and policy functions of the Radiocommunication Sector are performed by World and Regional Radiocommunication Conferences and Radiocommunication Assemblies supported by Study Groups.

Policy on Intellectual Property Right (IPR)

ITU-R policy on IPR is described in the Common Patent Policy for ITU-T/ITU-R/ISO/IEC referenced in Annex 1 of Resolution ITU-R 1. Forms to be used for the submission of patent statements and licensing declarations by patent holders are available from http://www.itu.int/ITU-R/go/patents/en where the Guidelines for Implementation of the Common Patent Policy for ITU-T/ITU-R/ISO/IEC and the ITU-R patent information database can also be found.

	Series of ITU-R Reports
	(Also available online at http://www.itu.int/publ/R-REP/en)
Series	**Title**
BO	Satellite delivery
BR	Recording for production, archival and play-out; film for television
BS	Broadcasting service (sound)
BT	**Broadcasting service (television)**
F	Fixed service
M	Mobile, radiodetermination, amateur and related satellite services
P	Radiowave propagation
RA	Radio astronomy
RS	Remote sensing systems
S	Fixed-satellite service
SA	Space applications and meteorology
SF	Frequency sharing and coordination between fixed-satellite and fixed service systems
SM	Spectrum management

Note: This ITU-R Report was approved in English by the Study Group under the procedure detailed in Resolution ITU-R 1.

Electronic Publication
Geneva, 2015

 ITU 2015

REPORT ITU-R BT.2382-0

Description of interference into a digital terrestrial television receiver

(2015)

TABLE OF CONTENTS

Introduction

Interference into a digital terrestrial television (DTT) receiver, i.e. violation of the protection ratio (PR), can impact the received picture. Section 1 describes the effects that limit the ability of DTT receivers from demodulating the wanted signal correctly. As digital broadcasting systems transmit source coded data, the relationship between demodulation failure and the visible picture impact is not as straightforward as it was in the case of analogue television and is described in Section 2.

Results of measurements for a specific interference case that illustrate its impact on the received picture are provided in the Annexes.

1   Interference on the RF level

Various effects can result in an interference into the signal decoded by a DTT receiver.

–   out-of-band emissions of the interferer which fall into the pass band of the receiver;

–   interferer in band emissions which are not attenuated enough by the receiver due to its limited selectivity;

–   environmental noise including man-made and impulse noise;

–   intermodulation in the receiver front-end;

–   channel multipath resulting in fading and intersymbol interference.

The impact to reception depends on which effects dominate.

1.1   Interfering transmitter out-of-band emissions

1.1.1   General Description

The interfering transmitter produces out of band emissions (OOBE) which are a result of signal processing, clipping and intermodulation. The level of OOBE depends on multiple factors such as the operational point of the amplifier, the modulation technique and filtering. Whilst equipment designs are not standardized, OOBE limits are part of a standards and specifications. Designers of RF equipment can then decide how to configure all the relevant parts of the equipment to achieve specified limits.

Depending on the type of interferer the interfering signal may be continuous or non-continuous (e.g. bursty or impulsive). This has a direct impact on the interferers OOBE. If the interferer is continuous the OOBE are continuous, i.e. the level of the additional "noise" into the receiver pass band is constant in time. If the interferer is 'bursty' the OOBE are 'bursty', i.e. the level of the additional "noise" into the receiver pass band varies with time getting close to gated noise.

1.1.2   Impact of OOBE interference on the receiver

Continuous OOBE impacts the receiver in a manner similar to additional (Gaussian) noise. However, the effect of 'bursty' OOBE cannot be as easily generalized.

In the case of 'bursty' interfering signal and the OOBE being well below the noise level of the receiver (e.g. $I/N = -10$ dB), the impact on the DTT receiver will be negligible. But in the case where the level of the OOBE exceeds the noise floor of the receiver the description of the impact cannot be easily described. On the one hand the interference which is only present for small fractions of time could be compensated by time interleaving (DVB-T2 only). The maximum fraction of time for the interference that a receiver can tolerate depends on the DTT FEC code rate, the depth of the time interleaver used in the transmitted DTT signal and the C/I ratio.

However, DVB-T has no time interleaver which means that for interference from OOBE which is only present for small fractions of the time it still degrades the received signal. This impact is the same for continuous and bursty transmission (see Annex 2 Table A2-2)

On the other hand, the demodulation of DTT signals relies on signal processing to ensure good performance. One input to the signal processing for example is the $C/(N+I)$ level of each data carrier. However, it has to be noted that the effect of bursty OOBE on the signal processing part is still not completely understood and may be subject to further studies.

1.2 Receiver adjacent channel selectivity

1.2.1 General Description

The receiver adjacent channel selectivity (ACS) is its ability to suppress signals outside its wanted channel. The ACS is often referred to as the filtering of the DTT receiver; however the receiver's ability to supress signals in the adjacent channel depends on all the receiver components. When deriving the ACS of a DTT receiver, demodulation and detection as well as error control coding performances of the receiver need to be taken into account. Measurements of PRs have shown that the AGC of the DTT receiver can play an important role for its selectivity.

Depending on the type of interferer the interfering signal may be continuous or non-continuous (bursty). This has an impact on the selectivity of the receiver.

1.2.2 Impact of ACS interference on the receiver

In the case of continuous interference the AGC can select its operational point correctly and the ACS of the receiver becomes solely a function of the filter.

For the case of 'bursty' interference the AGC faces a tricky situation for setting the operational point.

Modern DTT receivers must adapt quickly to impulsive interference to prevent saturation. Subsequent gain changes should be gentler to prevent modulation of the wanted signal by the AGC. To achieve this, AGC circuits with fast attack times (~1 ms) and slow recovery times (~150 ms) are often used. When a high level interferer is presented to the tuner, a rapid reduction in gain is applied to prevent overload. This can result in reduced sensitivity as the noise figure of the receiver is increased as a consequence of the gain reduction. This can furthermore result in an extended failure period after the interferer is removed while the AGC recovers and restores the front-end gain (sometimes known as "gain ducking").

This last effect can be overcome by improving the receiver ACS by, for example, the installation of a suitable filter (See Annex 2 Tables A2-1 and A2-2).

Time interleaving when used (e.g. DVB-T2) can reduce the impact of short burst interference, but can also, in certain circumstances, broaden the impact of an interference event to the duration of the interleaving frame.

The AGC time constant can cause failure of demodulation until the AGC circuit has recovered (reached its stable point).

1.3 Environmental noise

1.3.1 General Description

Environmental noise may come from various sources both natural and man-made. Atmospheric noise is produced mostly by lightning discharges. Galactic noise is caused by disturbances originating outside the earth and its atmosphere. Man-made noise consists of signals from unidentified

communication systems as well as various electrical equipment such as electric motors, transformers, heaters, lamps, ballast, power supplies, etc.

1.3.2   Impact of noise

Environmental noise impacts DTT reception by requiring higher DTT signal levels in order to maintain a minimum signal-to-noise ratio at the receiver. Additional information on environmental noise can be found in Report ITU-R BT.2265 and Recommendation ITU-R P.372.

1.4   Intermodulation in the receiver

1.4.1   General Description

The production, in a nonlinear element of a system, of frequencies corresponding to the sum and difference frequencies of the fundamentals and harmonics thereof that are transmitted through the element.

1.4.2   Impact of intermodulation

A nonlinear circuit or device that accepts as its input two different frequencies and presents at its output (a) a signal equal in frequency to the sum of the frequencies of the input signals, (b) a signal equal in frequency to the difference between the frequencies of the input signals, and, if they are not filtered out, (c) the original input frequencies

1.5   Signal Multipath

1.5.1   General Description

Signal multipath is a propagation phenomenon that results in a DTT signal reaching the receiving antenna by two or more paths. Causes of multipath include atmospheric ducting, ionospheric reflection and refraction, and reflection from terrestrial objects, such as mountains and buildings.

1.5.2   Impact of multipath

The effects of multipath include constructive and destructive inter-symbol interference, attenuation and phase shifting of the signal. Inter-symbol interference results when one symbol interferes with subsequent symbols and has a similar effect as noise. Annex 3 describes various cases of multipath interference.

2   Picture degradation of source coded video/audio data

2.1   Introduction

Digital Terrestrial Television is planned to provide a service that is quasi error-free (QEF). This is taken to mean no more than one bit error per hour[1]. Various methods are used within a typical broadcast TV network to achieve this, such as very robust Forward Error Correction that can correct bit errors to a quasi-error free (QEF) bit-stream, and the use in DVB-T2 of time interleaving to provide protection against impulsive interference. Depending on codec performance when such error correction fails, it could result in a visible or audible impairment to picture or sound respectively.

---

[1] The CEPT Chester 1997 agreement, for example, says "Quasi error-free means less than one uncorrected error event per hour, corresponding to BER = 1. 10^{-11} at the input of the MPEG-2 de-multiplexer." (Note 1 to Table A1.1.)

These impairments are of a finite duration, and evidence suggests that viewers' tolerance to them is low, particularly when they are accustomed to error-free reception.

2.2   Degradation of DTT

It is important to note the relationship between actual interference events and the impairment measures given above. Specifically, there is no one-to-one relationship between interference at the RF level and picture impairments. Some interference events may generate no visible errors, while others may generate visible errors that last much longer than the actual interference. The mechanisms for each of these are due to the underlying baseband processing, video coding and multiplexing employed in the DVB-T and DVB-T2 standard.

2.3   Time interleaving

A feature of DVB-T2 designed to overcome very short impulse interference is time interleaving. When this baseband processing technique is used, the bit-stream is "scrambled" in time in a known way before transmission, and "unscrambled" on reception. The effect of this is to reduce the impact of a short burst of interference by decreasing the likelihood that it will cause serious unrecoverable impact to any individual data component in the multiplex. For example, in the UK the DVB-T2 multiplex is operated with an interleaving depth of 20 symbols, i.e. 78 ms.

It should be noted that DVB-T transmissions use no time interleaving.

2.4   Video coding

In a typical HD TV scenario, an uncompressed video sequences (1 920 × 1 080i pixels@ 25 frames per second) are sampled and quantised at a data rate of 829 Mb/s (1 920 × 1 080 × 25 × 16 bit/s). Clearly, this is an impractical amount of data to transmit, so sequences are compressed to around 8 Mbit/s (or 1% of the original data rate) for broadcast by exploiting spatial and temporal redundancy in the video. The video frames are typically encoded as groups of pictures (GOPs) with a sequence length of typically 24-36 frames. Each GOP sequence commences with an I-frame (intra-encoded), which provides the necessary entry point for video decoding. All subsequent frames in the GOP are then encoded as motion compensated differences relying on interpolation from locally decoded reference frames. The reference frames are either previous frames (P-frames) or pairs of future and past frames (B-frames). Disruption to a frame within the GOP can result in a disturbance that may propagate as far as the next error-free I-frame. As the I frames occupy significantly more data capacity than the motion-compensated difference frames (B or P), there is a high probability that a short interference event will corrupt an I-frame, causing error propagation lasting until the I-frame in the next GOP. Severe errors can result in a need for the decoder to resynchronise, which may take over one second.

2.5   Video multiplexing

As a DVB-T2 channel can carry up to 40 Mbit/s of payload data, several video streams can be multiplexed into one channel. In theory, a short burst of interference might cause degradation to data for a service other than the one being watched, resulting in no visible picture impairment. In practice, the likelihood of this is determined by the length of the interference and the details of the multiplexing.

2.6 Visibility of Bit-Errors

An experiment was conducted[2] to estimate the likelihood of perceiving a single erroneous packet (188 bytes) in a DVB transport stream (TS) with MPEG 2 encoded material. It was found that losing a just single packet can lead to visible picture impairments. The chance of visibly degrading the video was found to be about 18%. However, in actual DTTB systems it is unlikely that the error will hit just one TS packet. This is due to multiple stages of interleaving. For example for 8k FFT DVB-T, the minimum interleaving length is about one ms which corresponds to the symbol duration.

3 List of Annexes

Measurements have been performed to illustrate certain interference effects or the combination thereof.

Annex 1 − The measurements in Annexes 1 have analysed how loss of signal due to AGC failure impacts the video and how long picture degradations are visible.

Annex 2 − The measurements in Annex 2 have analysed the impact of in band (IB) and out-of-band (OOB) emissions of discontinuous (bursty) interference on DTT reception (DVB-T and DVB-T2) for different receiver selectivity.

Annex 3 − The measurements and analysis in Annex 3 illustrate various scenarios of multipath interference.

---

[2] Reibmann A, Kanumuri S, Vaishampayan V, Cosman P (2004) *Visibility of individual packet losses in MPEG-2 video*, IEE International Conference on Image Processing (ICIP), 1:171-174.

Annex 1

Duration of picture degradation resulting from
a very short burst of interference

1 Introduction

Broadcast systems have no mechanism to re-transmit corrupted data. Instead, the corrupted data will propagate through the broadcast receiver resulting in degradation to the AV content. This process is referred to as error extension. An understanding of this mechanism is important when assessing the impact. This Annex illustrates what happens to the video when the receiver experiences interference, i.e. the channel decoder of the receiver was not able to repair the damaged bit stream. In particular, it is shown that a very short burst of interference will lead to picture degradations which are significantly longer than the duration of the interference burst.

2 Study 1

2.1 Setup

The set-up was chosen to show the effect of picture degradation beyond the time duration of interference at the RF level. This means that the results are not related to the impact of specific values of ACS and ACLR on DTT receiver performance.

Table A1-1 lists the equipment which was used in the tests.

TABLE A1-1

Equipment List

Type	Model
Pulse generator	HP
Broadband signal generator	Rohde & Schwarz SMU 200A Constant 10 MHz broadband signal
DVB-T/T2 signal generator	Rohde & Schwarz SFU DVB-T2 settings: UK Mode 40.21 Mbit/s 256QAM, CR=2/3, PP7, GI=1/128 202 FEC blocks per interleaving frame TI blocks per frame: 3 T2 frame per interleaving frame: 1 Frame interval: 1 Type of interleaving: 0 Time interleaving length: 3
Real time spectrum analyser	Tektronix RSA 6114A
Spectrum analyser	Rohde & Schwarz FSQ8
Remote controlled RF switch	PIN diode switch
DVB-T2 receiver	2 DVB-T2 Set-Top-Boxes (A, B)

Figure A1-1 shows the test setup as it was used for the measurements.

FIGURE A1-1

Test setup
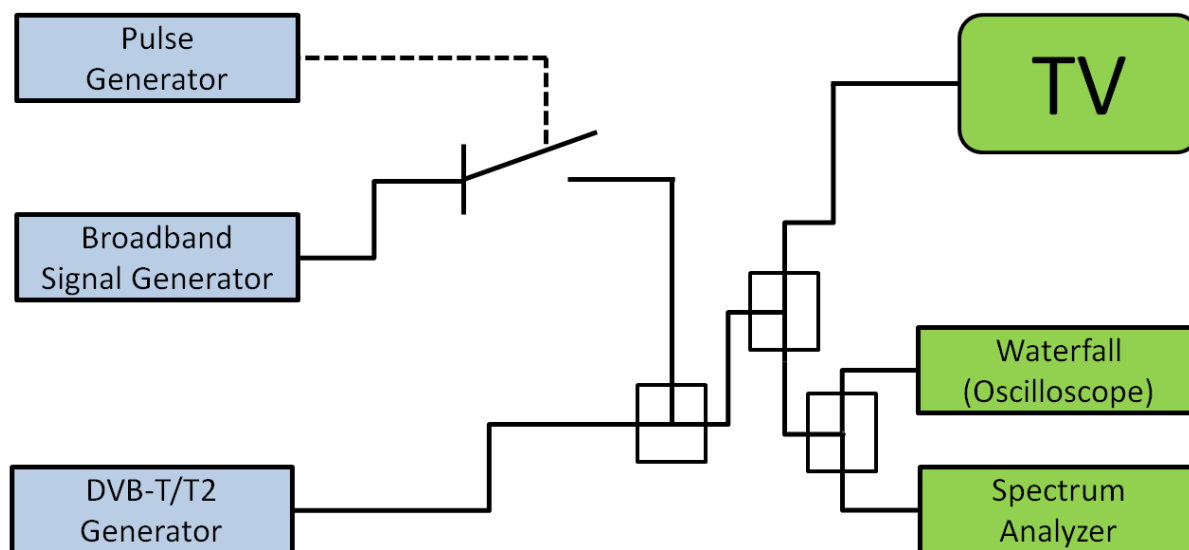
The DVB-T/T2 Generator was set according to the current UK DVB-T2 specifications using original UK content; a multiplex containing 4 HD video streams and associated data. For these tests the BBC One HD and Channel 4 HD video streams were used to ensure realistic signal properties.

The frequency setting corresponded to a scenario of a 9 MHz Guard Band. The DVB-T2 frequency was centred at 690 MHz (channel 48) and the LTE signal (10 MHz block) was centred at 708 MHz.

The DVB-T2 input signal level at the TV was –72 dBm which is about 10 dB above the minimum level.

The DVB-T2 signal was combined with a 10 MHz LTE interfering signal produced by the broadband signal generator. This interfering signal was switched on and off by the PIN-Diode RF-switch controlled by the pulse generator. The interferer level at the TV was set one dB above the level where constant interference caused the picture to fail. For the two receivers under test, this meant that every interference pulse could cause bit-stream errors which might not be corrected.

The protection ratios found for constant interference are listed in Table A1-2.

TABLE A1-2

DVB-T2 protection ratio for continuous interference

Set-top-box	Protection ratio/dB (cont.)
A	–47
B	–48

The TV picture was recorded with a camera to document the effects of such interference. Based on the video frames with visible picture errors the error duration was calculated.

Test patterns

The interference patterns, i.e. pulse repeat frequency, listed in Table A1-3 were tested.

TABLE A1-3

Test pattern

Case #	Purpose	Period	Impulse length	Proportion of interference at RF level
1	Production of illustrative videos of one minute duration to show the interference impact	1 s	1 ms	0.1%
2	Analysis of the duration of the impact on the TV picture	5 s	1 ms	0.02%

Figure A1-2 visualizes the temporal structure of the two test patterns.

FIGURE A1-2

Pulse pattern for Cases #1 and #2
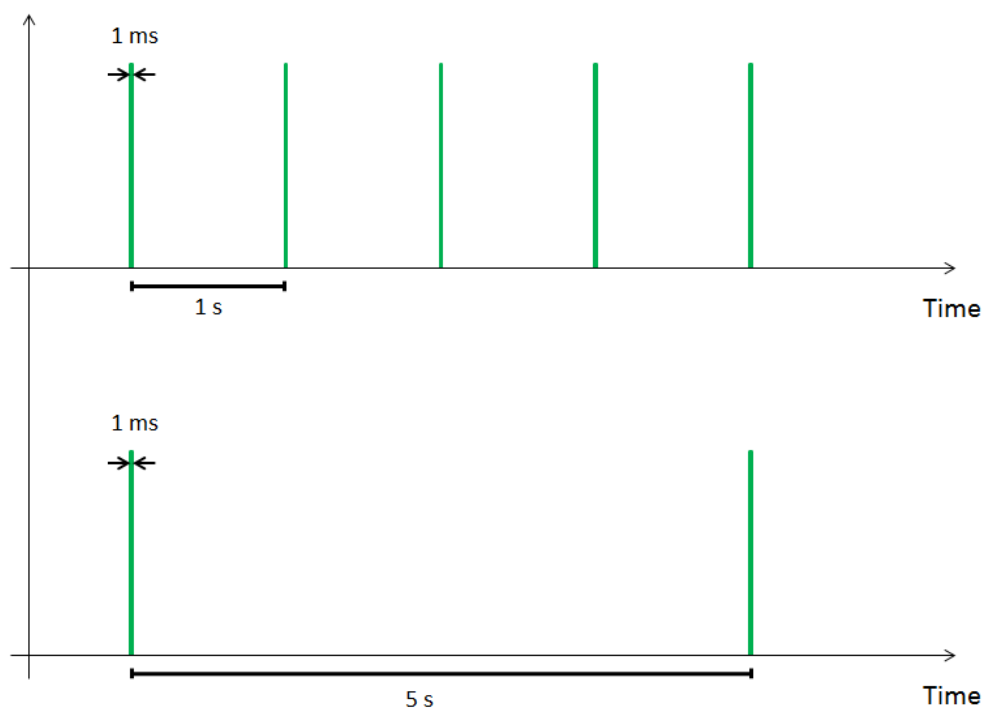
2.2 Results

2.2.1 Set-top-box picture error type

Set-top-box A tries to freeze the picture during the duration of picture errors (masking). Set-top-box B just shows the decoded errors with no masking. The distorted slices are always visible and quite disturbing to the viewer.

2.2.2   Results for test Case #1

Box A tries to mask picture problems by stopping the video flow. However, that can be quite annoying as can be seen in the following video:

Box A BBC.mp4

Box B however, does show all picture errors as can be seen in the video below. This does not stop the flow of pictures, but here the affected parts of the picture are much more visible.

Box B BBC .mp4

2.2.3   Results for test Case #2

2.2.3.1   Set-top-box A

FIGURE A1-3

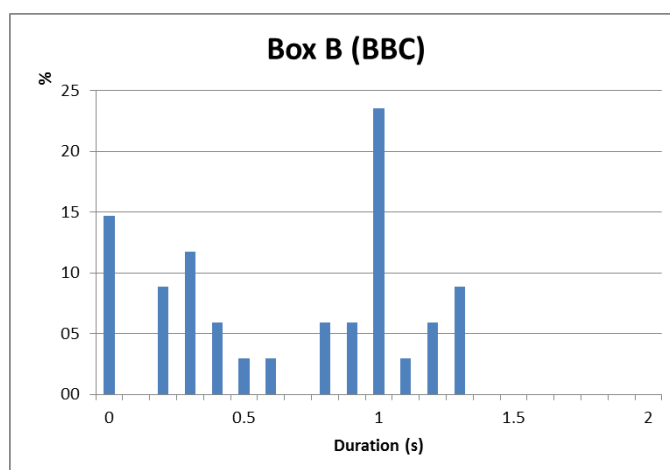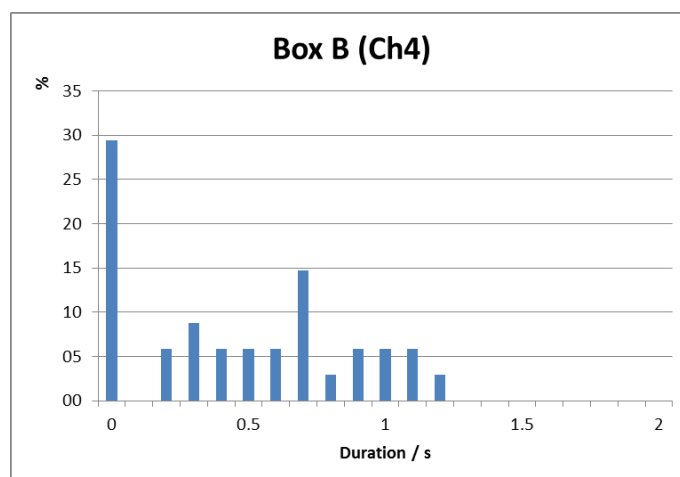**Box A – Distribution of error duration – BBC one HD**
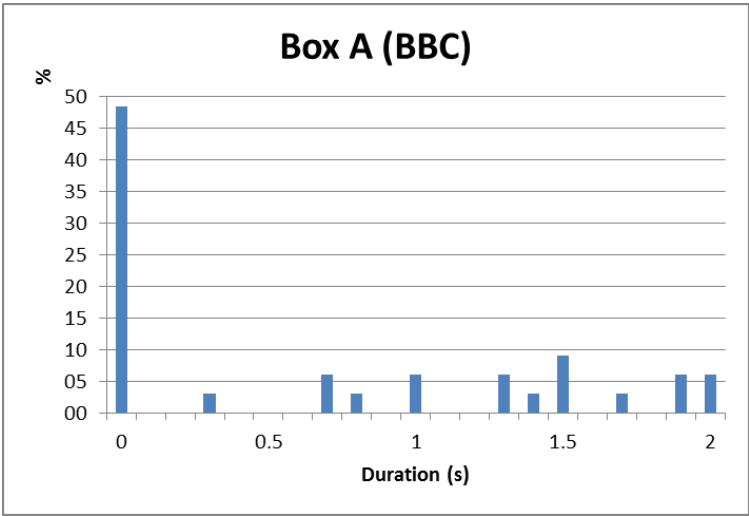
FIGURE A1-4

Box A – Distribution of error duration – Channel 4 HD
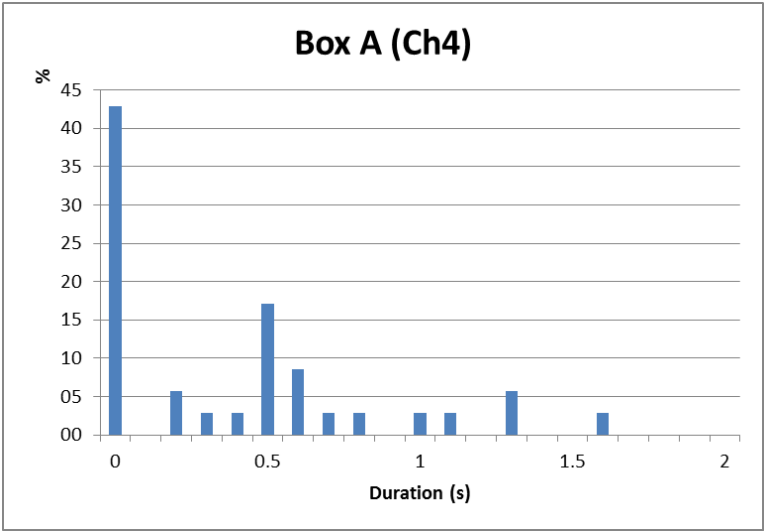
The first column with 0 s duration means that the interference pulse had no visual impact. The difference in distribution of duration of errors between Figs A1-3 and A1-4 is due to different content. Figure A1-3 relates to content where long scenes appeared and changes were slow whereas Fig. A1-4 relates to quickly changing scenes.

It is also shown that if an error occurs it lasts at least 0.2 s.

2.2.3.2   Set-top-box B

FIGURE 5

Box B – Distribution of error duration – BBC one HD

FIGURE 6

Box B – Distribution of error duration – Channel 4 HD

The first column with 0 s duration means that the interference pulse had no visual impact. The difference in distribution of duration of errors as well as the higher number of longer lasting picture degradation between Fig. A1-5 and Fig. A1-6 can be explained due to different content. Figure A1-5 relates to content where long scenes appeared and changes were slow whereas Fig. A1-6 relates to quickly changing scenes.

It is also shown, that if an error occurs, it lasts at least 0.2 s.

2.2.3.3   The median duration and the standard deviation of the occurred picture degradation

Table A1-4 shows the statistical analysis of the results shown in Figs A1-3 to A1-6. The 0s cases, i.e. no impact could be detected have not been considered when deriving mean and standard deviation.

TABLE A1-4

Median duration and the standard deviation of errors occurred

Set-top box	BBC One HD		Channel 4 HD	
	Median	**Std Dev**	**Median**	**Std Dev**
A	1.3 s	0.6 s	0.7 s	0.4 s
B	0.8 s	0.4 s	0.7 s	0.3 s

2.2.4   General description of the picture error effect

Degradation of the picture happens because the TV receiver could not correct the errors caused by the interference on the RF level. A part of the bit stream is corrupted. The video decoder then misses information to properly build the picture which can then become noticeable for the viewer.

It has to be noted that the type and severity of the picture degradation depends on the part of the data that is affected as well as on the separation of I-Frames. Video material with frequent shot changes reduces the subjective impact and to some extent can even hide it. This is due to adaptive coding, variable GOP (Group Of Pictures) length, etc.

2.3   Conclusion

The measurements have shown that if a TV receiver experienced harmful interference at the RF level this can lead to long lasting picture errors. As a rule of thumb it can be said that very short RF interference leads to around one second of picture errors.

3   Study 2

3.1   Experimental method

A pulsed LTE interferer and a wanted DTT signal were applied to a DTT receiver. The wanted signal was set to a level of –70 dBm corresponding to a fade margin of 10 dB. The level of the interference was adjusted to the onset of picture failure, typically 40-50 dB above the wanted DTT signal at a frequency offset of 18 MHz. The test arrangement is shown in Fig. A1-7 below.

FIGURE 7

Laboratory test configuration
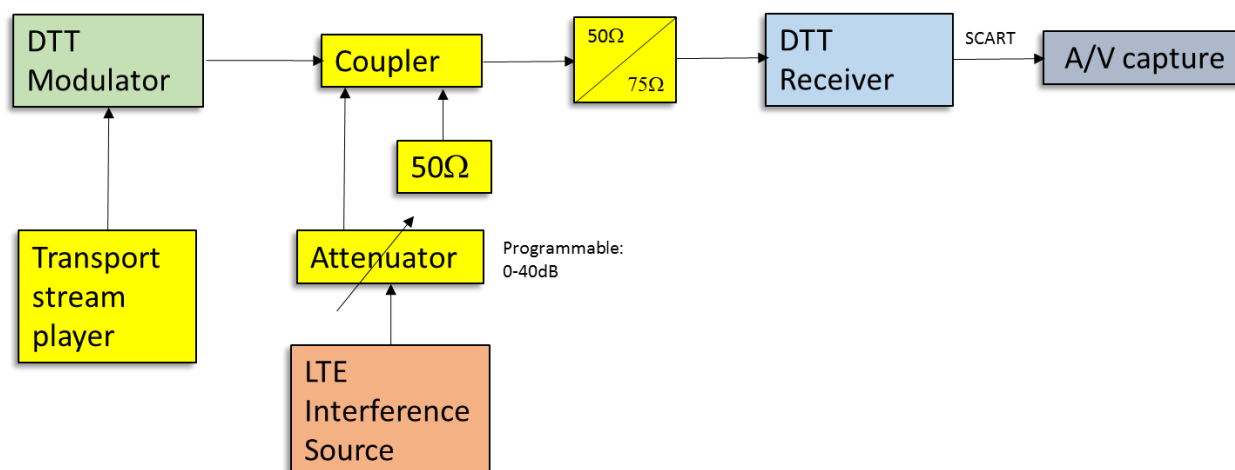
3.2 DTT test signal

The DVB-T2 mode used in the UK was used for the tests (256-QAM, FEC Rate 2/3, GI 1/32, 40 Mb/s Capacity). The transport stream included 4 HD programme streams (1 920 x 1 080 pixels) each of approximately 8-10 Mb/s capacity. The video services are encoded using H.264 with statistical multiplexing which allows the individual programme streams a variable fraction of the total transport stream capacity.

3.3 LTE test signal

For these tests an RF vector signal generator equipped with a baseband arbitrary function generator (R&S SFU) was used. The IQ test signal used to drive the vector signal generator was generated using MATLAB. A recording from an LTE terminal was processed to extract the IQ data corresponding to an active LTE resource block pair (~1 ms duration). This sequence was then padded with zeros resulting in a one ms pulse applied every 5 seconds. The characteristics of the waveform are show in Figs A1-8, A1-9 and A1-10. These Figures were captured using a R&S FSV spectrum analyser.

FIGURE A1-8

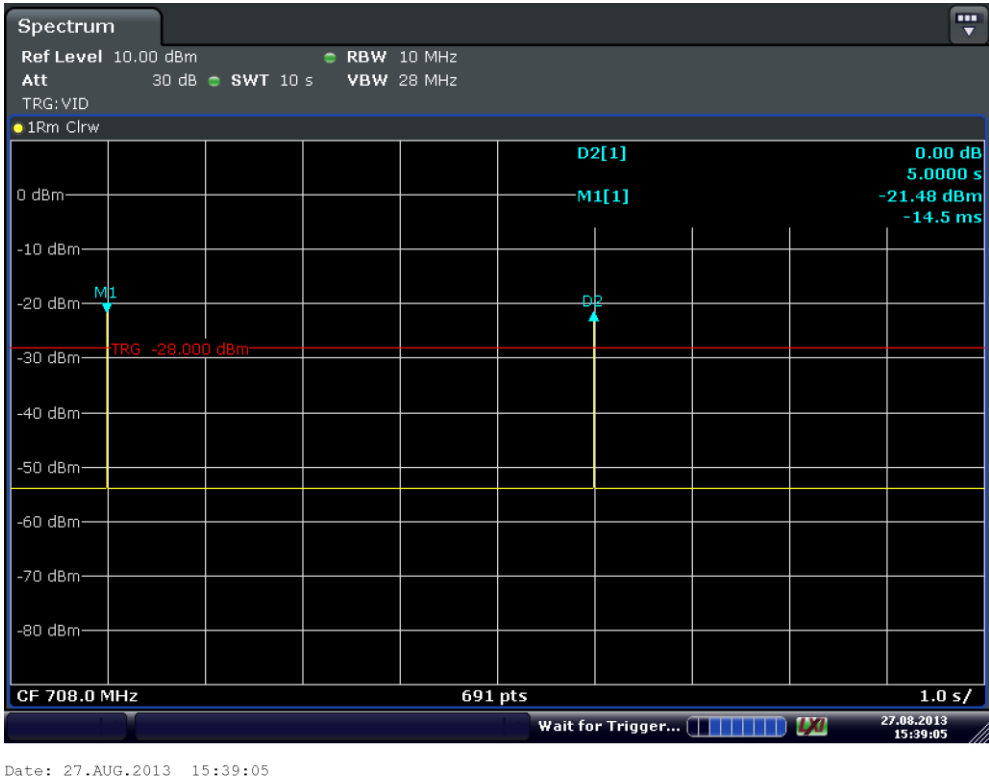**Spectrum analyser trace showing 5 second pulse repetition**

Date: 27.AUG.2013   15:39:05

FIGURE A1-9

Spectrum analyser trace showing 5 second pulse repetition
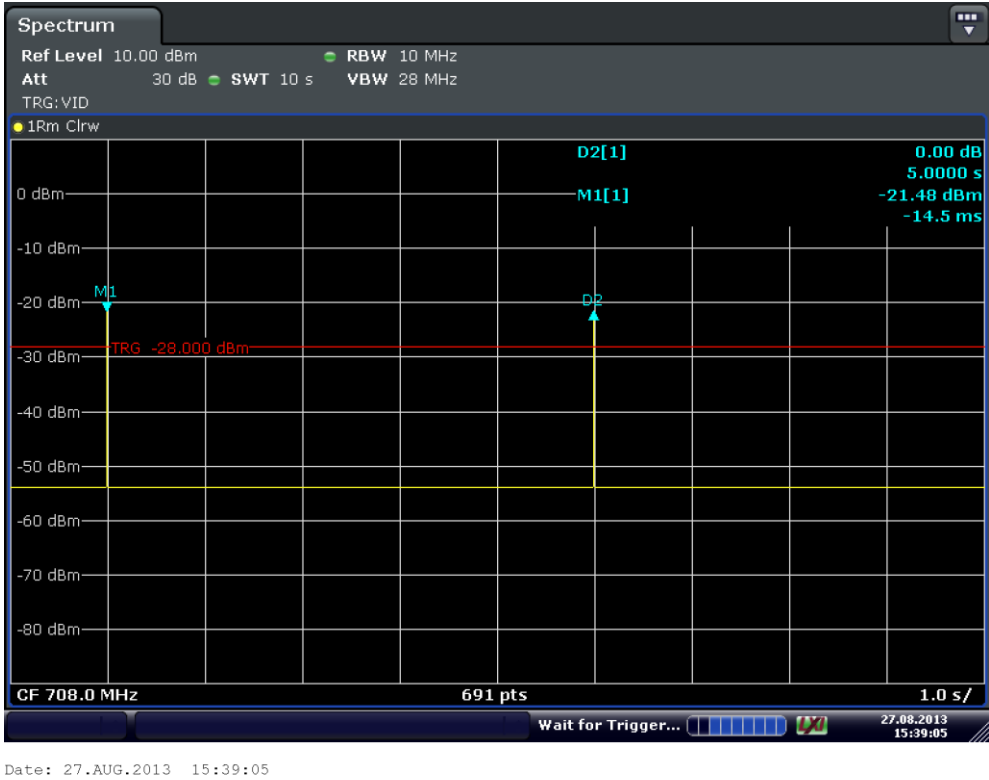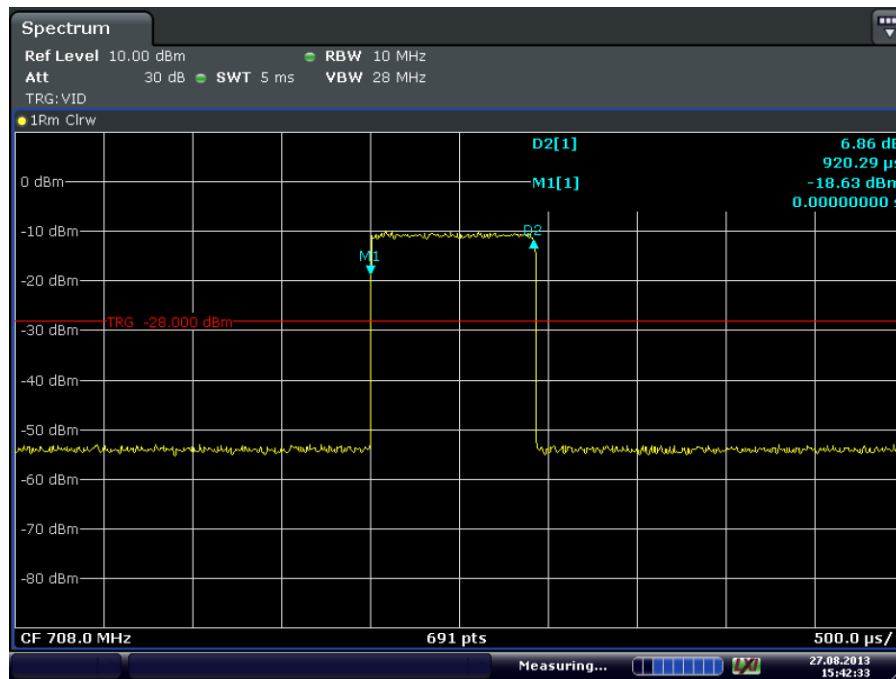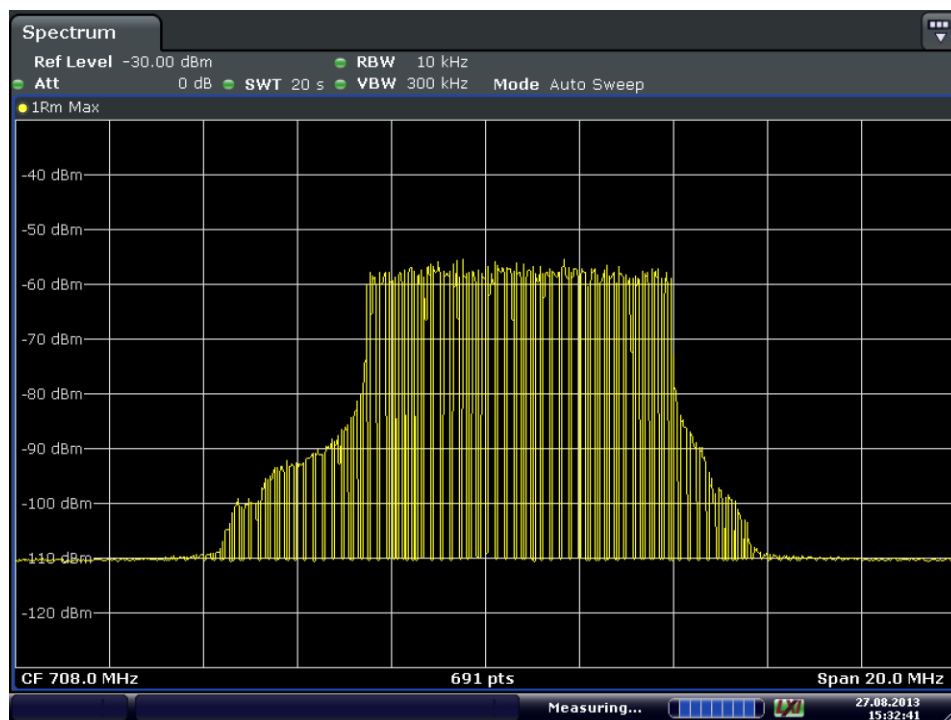

Date: 27.AUG.2013   15:39:05

FIGURE A1-10

Spectrum Analyser Trace Showing Detail of LTE Pulse

Date: 27.AUG.2013 15:42:33

FIGURE A1-11

Spectrum of LTE UE Pulse

Date: 27.AUG.2013 15:32:41

### 3.4	Results

The decoded video shows a varying level of disruption to the video with error extension up to 2 seconds in duration. Although the interference pulse is active for a tiny fraction of the video frame, disturbance of the picture can extend over many frames. The disturbance can affect the entire video frame or just a small proportion of the picture depending on which part of the coded video is impacted.

FIGURE A1-12

Video frame with extensive impairment

FIGURE A1-13

Video frame with localised impairment

3.5 Analysis

The distribution of the error extension can be analysed by measuring the duration of the impairment for each event and plotting a histogram showing the spread in the interval length.

The histogram for receiver A is shown in Fig. A1-14.

FIGURE A1-14

Distribution of video impairment duration for receiver A
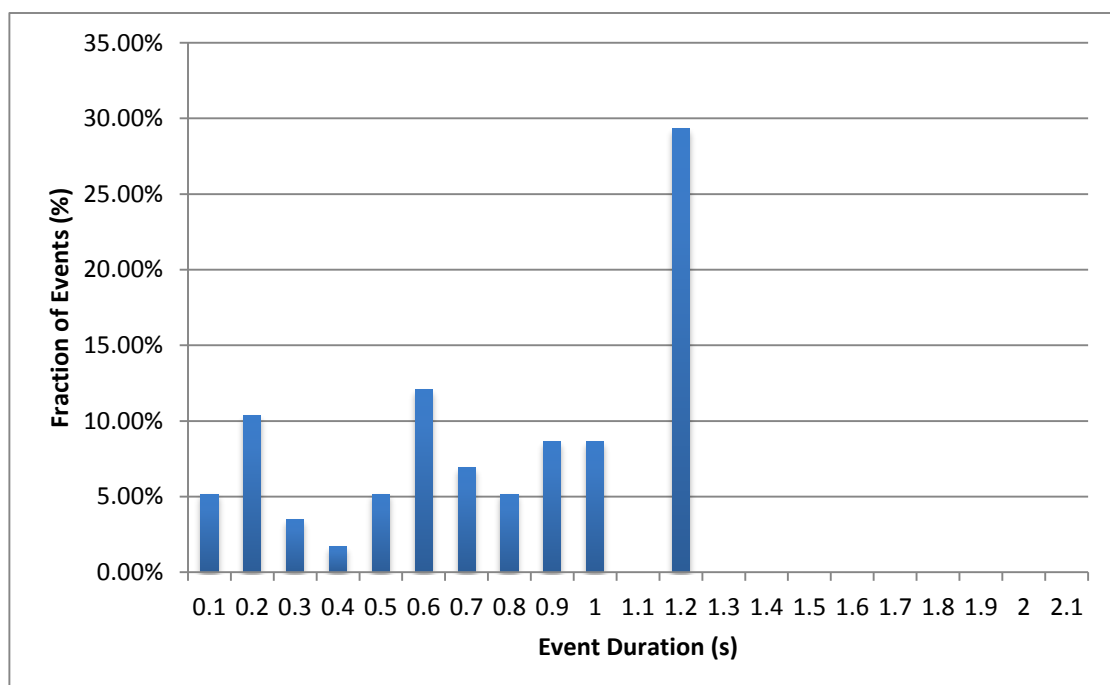
The maximum duration observed was 1.2 seconds. The nominal GOP length of the coded video is known to be 24 frames, which can be extended to 32 frames if the next I frame in the GOP falls within 8 frames of a shot change.

The histogram for receiver B is shown in Fig. A1-15.

FIGURE A1-15

Distribution of video impairment duration for receiver B
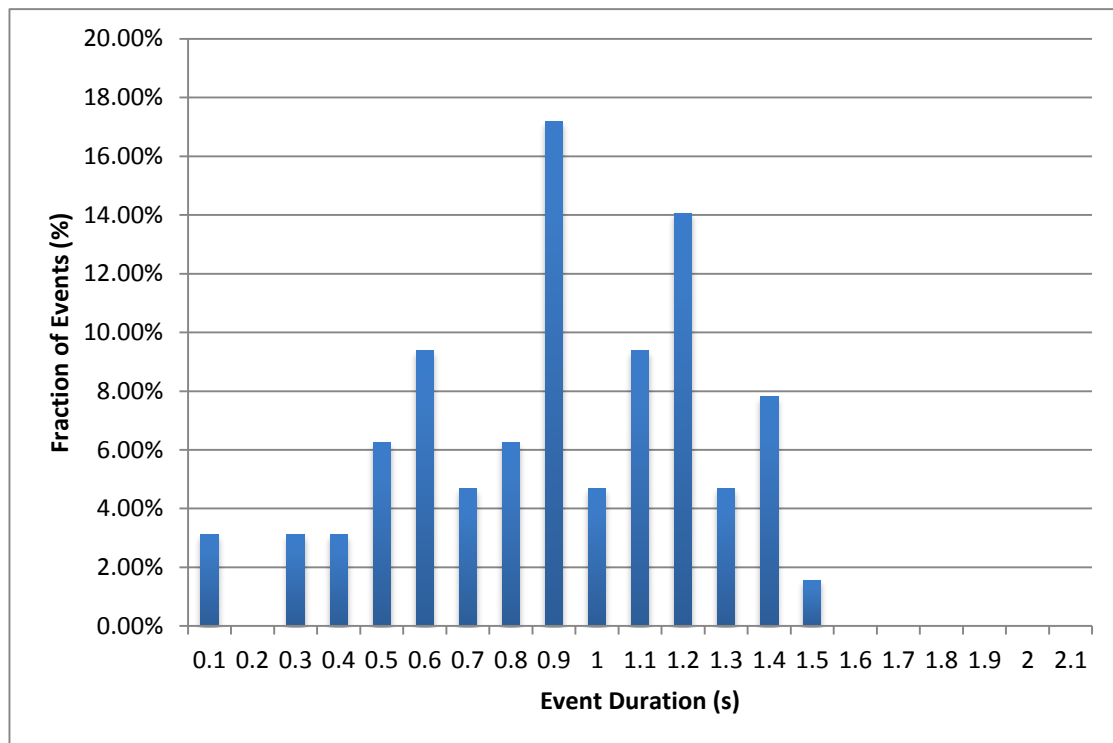
Receiver B is known to suffer with AGC related issues and shows increased error extension compared to receiver A.

3.6   Discussion

There are a number of interacting mechanisms which can result in the observed error extension.

It should be noted that the original uncompressed video sequences (1 920 × 1 080i pixels@ 25 fps) are sampled and quantised at a data rate of 829 Mb/s (1 920 × 1 080 × 25 × 16 b/s). The sequences have been compressed to 8 Mb/s (1%) for broadcast by exploiting spatial and temporal redundancy in the video. The video frames are typically encoded as groups of pictures (GOPs) with a sequence length of typically 24 – 36 frames. Each GOP sequence commences with an I (intra-encoded) frame, which provides the necessary entry point for video decoding. All subsequent frames in the GOP are then encoded as motion compensated differences relying on interpolation from locally decoded reference frames. The reference frames are either previous frames (P-frames) or pairs of future and past frames (B-frames). Disruption to a frame within the GOP can result in a disturbance that may propagate to the next error-free I-frame. As the I frames occupy significantly more data capacity than the motion compensated difference frames (B or P), there is a high probability that a short interference event will corrupt an I-frame, causing error propagation lasting until the I-frame in the next GOP.

Severe errors can result in a need for the decoder to resynchronise, which in the worst case may take up to one second.

A further source of error extension is the AGC characteristics of the RF tuner. Modern DTT receivers must adapt quickly to short bursts of interference to prevent saturation. Subsequent gain changes should be gentler to prevent modulation of the wanted signal by the AGC. To achieve this, AGC circuits with fast attack times (~1 ms) and slow recovery times (~150 ms) are often used. When a high level interferer is presented to the tuner, a rapid reduction in gain is applied to prevent overload. This can result in reduced sensitivity as the noise figure of the receiver is increased as a consequence of the gain reduction. This can result in an extended failure period after the interferer is removed while the AGC recovers and restores the front-end gain (sometimes known as "gain ducking").

3.7 Conclusions

These tests show extensive error extension to DTT resulting from short bursts of interference on two DTT receivers. Possible mechanisms for the observed error extension have been discussed and include propagation of errors through the H.264 GOP sequence and interaction with DTT tuner AGC circuits. Such mechanisms appear to contribute to the observed error extension of up to 1.5 seconds.

Annex 2

Assessment of the impact of OOBE as well as short pulse interferences from IMT user equipment to DTTB reception

1   Introduction

This report presents the results of the measurements carried out on ten different DTT receivers (DVB-T 64 QAM and DVB-T2 256 OAM receivers) available on the European market, for assessing the impact of short pulse interferences from IMT (LTE) user equipment to DTT reception on adjacent channel (DTT receiving below 694 MHz and IMT(LTE) uplink starting at 703 MHz). The experimentation aims at providing information on the co-existence of DTT broadcasting with IMT user equipment and on the general assessment of interference into a DTT receiver from the type of emission typical from IMT (LTE) user equipment.

The SFP (subjective failure point) assessment was used for determining the DTT protection ratios. The detailed measurement method and parameters can be found in Report ITU-R BT. 2215-4.

2   Summary of the used measurement methodology

2.1   Test set-up used

The test setup for protection ratio and overloading threshold measurements is depicted in Fig. A2-1.

FIGURE A2-1

Measurements set-up
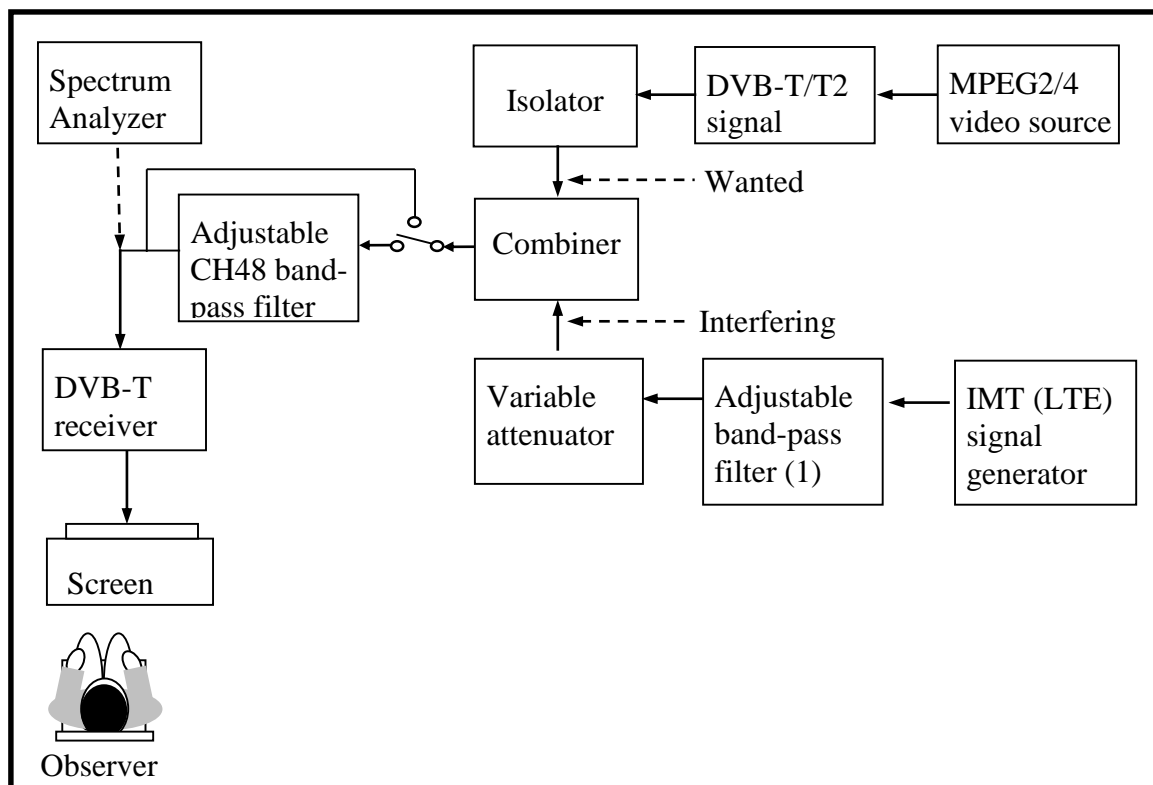
An adjustable band-pass filter (1) was inserted between the interfering signal generator and the combiner. The objective of this filter is to eliminate the wideband noise generated by the interfering signal generator and adjust the interfering signal to the correct interference transmission mask and ACLR values. An isolator was also inserted between the DVB-T signal generator and the combiner to keep the power from the interfering signal generator returning to the DVB-T signal generator output.

A CH48 BPF (2) has been used to reduce the UE in band (IB) emissions falling into DTTB CH48 and consequently to identify the predominate component of the interfering UE emissions, which are composed of UE IB and OOB emissions, on the DTTB reception

2.2 Frequency offsets between IMT UE interfering signal and DTTB wanted signal

A single frequency offset has been used (18 MHz) aiming at limiting the number of measurement to be carried out. This frequency offset corresponds to a guard band (GB) of 9 MHz between DTTB centred at 690 MHz and the IMT UE signal centred at 708 MHz as shown in Fig. A2-2.

FIGURE A2-2

Frequency offsets between IMT UE and DTTB signals
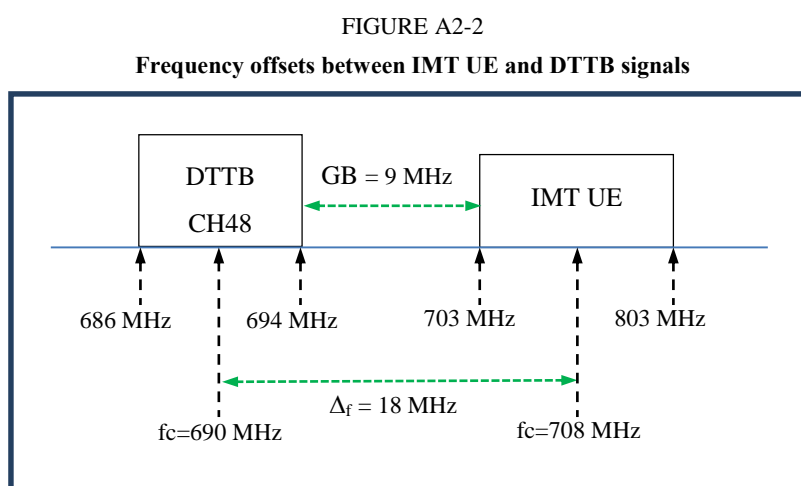
2.3 Generation of the IMT uplink signals

The uplink signal can vary considerably in both the time and frequency domains depending upon the traffic loading required. In the frequency domain the number of RBs allocated for each SC-FDMA symbol can vary rapidly. The number of RBs is 50. In the time domain, there can be long periods where the UE does not transmit at all, leading to an irregular pulse like power profile.

In this measurement campaign three different UE transmission modes have been used:

– Continuous transmission (TM1);

– Discontinuous transmission (TM2) with: UE signal maximum transmission duration = 1 ms, transmission period = 1 s; [3]

– Discontinuous transmission (TM3) with: UE signal maximum transmission duration = 1 ms, transmission period = 5 s. [3]

---

[3] This type of interference signal was chosen to illustrate certain effects with a well-defined and reproducible signal.

The UE generator output power was fixed to 20.83 dBm. Two different ACLR values, 60 and 70 dB, have been used in measurements. These ACLR values were obtained by means of an inline band pass filter (BPF) on UE signal generator. They correspond respectively to –37 and –47 dBm/8 MHz, for an IMT UE maximum transmit power of 23 dBm, in case of full uplink resource allocation (50 RBs).

The time domain shape of the signal TM2 is shown in Fig. A2-3.

FIGURE A2-3

**IMT UE TM2 signal having an ACLR of 60 dB on the time domain.
Detail of several pulses**
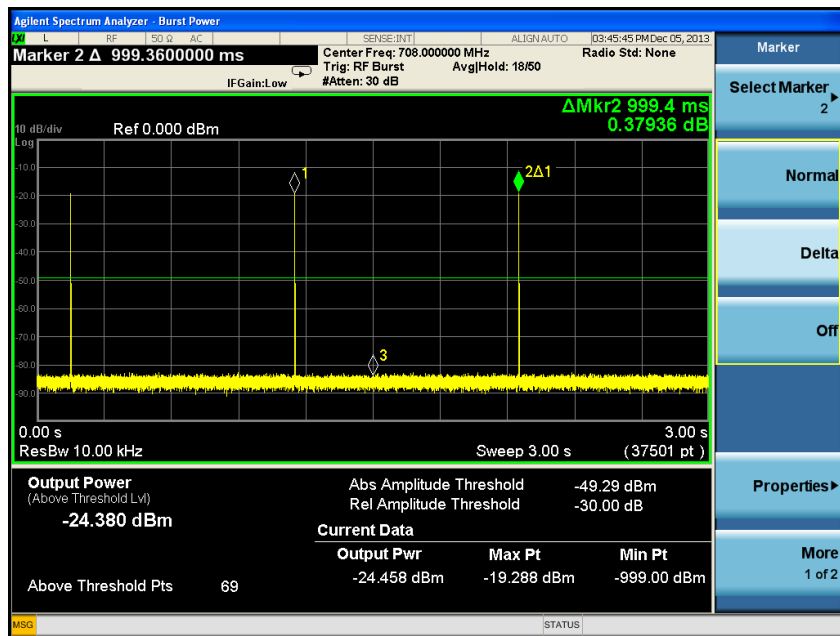
A CH48 BPF has been used to reduce the UE in band (IB) emissions falling into DTTB CH48 and consequently to identify the predominate component of the interfering UE emissions, which are composed of UE IB and OOB emissions, on the DTTB reception.

Measurements were carried out in two steps, for UE $ACLR_{CH48}$= 60 and 70 dB, with full IMT UE resource allocation (50 RBs):

➢   C(I) of the DTTB receiver under test were measured for UE TM1, without and with an inline external CH48 BPF filter on the DTTB receiver input;

➢   C(I) of the DTTB receiver under test were measured for UE TM2 and TM3, without and with an inline external CH48 BPF filter on the DTTB receiver input.

The objective of these measurements is to evaluate the impact of the UE OOBE and IBE on DTTB PR and Oth respectively in case of a continuous (Step 1) as well as in case of a discontinuous (Step 2) IMT UE emission.

The IMT UE signal was attenuated by CH48 BPF by 36 dB. The insertion loss of the filter over DTTB channel 48 was 3 dB. Consequently, the effective ACS improvement of DTTB receivers by the filter was about 33 dB.

3 Measurement results and conclusions

The detailed measurement results are provided in Report ITU-R BT. 2215-4.

3.1 Analysis of the measurement results

Measurement results are summarised in Tables A2-1 and A2-2.

TABLE A2-1

DVB-T2 receivers' average protection ratios			
Average ACS without filter = 65 dB, Average ACS with CH48 BPF = 98 dB			
Continuous Tx ACLR=60 No Filter	**Continuous Tx, ACLR=60 CH48 BPF**	**Continuous Tx, ACLR=70 No Filter**	**Continuous Tx, ACLR=70, CH48 BPF**
Average PR (dB)	Average PR (dB)	Average PR (dB)	Average PR (dB)
–42	–43	–45	–54
Average Oth (dBm)	Average Oth (dBm)	Average Oth (dBm)	Average Oth (dBm)
–3	NR	–3	NR
DVB-T2 receivers			
Average ACS without filter = 65 dB, Average ACS with CH48 BPF = 98 dB			
Discontinuous Tx, ACLR=60 No Filter	**Discontinuous Tx, ACLR=60 CH48 BPF**	**Discontinuous Tx, ACLR=70 No Filter**	**Discontinuous Tx, ACLR=70, CH48 BPF**
Average PR (dB)	Average PR (dB)	Average PR (dB)	Average PR (dB)
–49	–70	–50	–72
Average Oth (dBm)	Average Oth (dBm)	Average Oth (dBm)	Average Oth (dBm)
NR	NR	NR	NR

TABLE A2-2

DVB-T receivers' average protection ratios			
Average ACS without filter = 62 dB, Average ACS with CH48 BPF = 95 dB			
Continuous Tx ACLR=60	Continuous Tx, ACLR=60 CH48 BPF	Continuous Tx, ACLR=70	Continuous Tx, ACLR=70, CH48 BPF
Average PR (dB)	Average PR (dB)	Average PR (dB)	Average PR (dB)
–40	–41	–43	–54
Average Oth (dBm)	Average Oth (dBm)	Average Oth (dBm)	Average Oth (dBm)
–2	NR	–2	NR
DVB-T receivers			
Average ACS without filter = 62 dB, Average ACS with CH48 BPF = 95 dB			
Discontinuous Tx ACLR=60	Discontinuous Tx, ACLR=60 CH48 BPF	Discontinuous Tx, ACLR=70	Discontinuous Tx, ACLR=70, CH48 BPF
Average PR (dB)	Average PR (dB)	Average PR (dB)	Average PR (dB)
–22	–42	–23	–53
Average Oth (dBm)	Average Oth (dBm)	Average Oth (dBm)	Average Oth (dBm)
–5	NR	–4	NR

Impact of continuous and discontinuous interfering signals on DTT reception:

The tested DTT (DVB-T and DVB-T2) receivers have behaved very similarly in the presence of a continuous IMT UE signal, while they have behaved very differently one from the other in the presence of a discontinuous (time varying) IMT UE signal. The ACS of the DTTB receivers tested was in the range of 62 to 65 dB. In the presence of a discontinuous IMT UE signal, modern DVB-T2 receivers, on average, have behaved well. Their protection ratios (PR) were 7 to 27 dB better than those measured in the presence of a continuous UE signal. At the opposite, the performance of DVB-T receivers was reduced by about 20 dB, compared to their performances in the presence of a continuous UE signal.

- **In the case of a continuous IMT UE signal**:
  - For receivers with an ACS of 62/65 dB, reducing the UE OOBE level from –37 dBm (UE ACLR = 60 dB) to –47 dBm (UE ACLR = 70 dB) has improved DTTB receivers' protection ratios only by about 3 dB.
  - For receivers with an ACS of 95/98 dB, when the ACS was improved by an external filter, reducing the UE OOBE level from –37 dBm to –47 dBm has improved DTT receivers' protection ratios by about 11 to13 dB.
- **In the case of a discontinuous IMT UE signal**:
  - for receiver ACS of 62/65 dB, reducing the UE OOBE level from –37 dBm (UE ACLR = 60 dB) to –47 dBm (UE ACLR = 70 dB) has improved DTT receivers' protection ratios only by one dB.
  - for receiver ACS of 95/98 dB, when the ACS was improved by an external filter, reducing the UE OOBE level from –37 dBm to –47 dBm:
    - has improved DVB-T2 receivers' protection ratios by only 2 dB;

    – has improved DVB-T receivers' protection ratios by 11 dB, PRs improved to their values in the presence of a continuous IMT UE signal.

  – for a given OOBE level (–37 or –47 dBm), improving the DTT receivers ACS by 33 dB (from 62/65 to 95/98):

    – has improved DVB-T2 receivers' protection ratios by about 18-27 dB compared to those measured in the presence of a continuous UE signal;

    – has not improved DVB-T receivers' protection ratios compared to those measured in the presence of a continuous UE signal.

3.2 Conclusions

On average, modern DVB-T2 receivers tested have behaved better in the presence of a discontinuous IMT UE signal than in the presence of a continuous IMT UE signal while the performance of DVB-T receivers was reduced by about 20 dB, compared to their performances in the presence of a continuous UE signal.

The reduction of the performance of DVB-T receivers (increase of their protection ratios) was due to the in band emissions (IBE) of the discontinuous UE signal and not due to its OOBE.

The impact of discontinuous IMT UE emissions on DTT reception can be efficiently combated by improving DTT receivers' AGC circuits, including the overall ACS of the receivers; improving only the ACLR (OOBE) of IMT UE signal does not improve significantly the PR of the receivers.

Finally, the values of ACLR and ACS should be similar in magnitude for obtaining the best performance in reduction and filtering of out of band emissions.

Annex 3

Field measurement and analysis of various multipath interference scenarios

1   Introduction

This Annex describes the measurement and analysis of real multipath propagation conditions found in the field. Field studies of ATSC DTV signal reception have demonstrated a wide range of varying multipath and noise conditions. It is generally admitted that there is no adequate model representing the diversity of conditions observed in the field. Past experience has proven that there is a clear benefit in gaining knowledge from the field environment to improve DTT reception.

A set of field ensembles from ATSC captured signals provides an example of the various conditions that can be observed in the field. Most of the field ensembles contain data captured at sites where reception was difficult. The field ensembles are clearly not meant to represent the statistics of overall reception conditions but rather to serve as examples of difficulties that are commonly experienced in the field. The field ensembles were recorded in the Washington, D.C., area and in New York City. The data includes outdoor and indoor captures of 25 seconds in different types of environments, such as rural, residential, and suburban areas. Details of the captures can be found in ATSC A/74, "ATSC Recommended Practice: Receiver Performance Guidelines".

The channel characteristics have been extracted from observations of the channel spectrum over the entire period of the capture. The impulse response estimate is produced by a correlation between the received signal and the PN511 binary training sequence embedded in the data field sync. The impulse response produces a channel estimate with a maximum echo span of −23 μs (for pre-echo) and + 23 μs (for post-echo) for every data field sync segment.

2   Impulse response analysis

This section provides a detailed impulse response analysis for a selection of captured field ensembles. The field ensembles were selected to give examples of the richness of multipath conditions in the field. The ensembles, however, do not necessarily represent limits on field conditions that may be experienced.

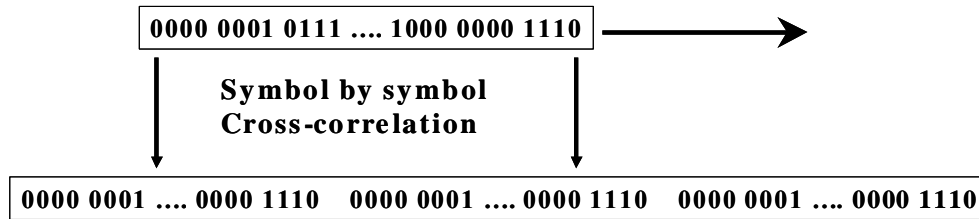## 2.1   Channel estimations using 511 Pseudo-Random Sequence

Channel estimations may be obtained from RF captures using the 511 pseudo-random number sequence located in the ATSC 8-VSB field sync. The field sync and its PN511 sequence is repeated every 24.2 milliseconds. Consequently, over 1000 channel estimations may be computed during each 25-second capture.

The channel estimation is calculated using a symbol-by-symbol cross-correlation of the recovered ATSC 8-VSB symbol stream. The PN511 symbol sequence is located within the synchronization segment of the captured RF signal. This recovered PN511 sequence is correlated with three ideal PN511 sequences, as illustrated in Fig. A3-1. As the recovered PN511 sequence is incremented across the ideal sequences, the main path and echoes are revealed in the results of the correlation.

FIGURE A3-1

**Method of channel estimation using the PN511 pseudo-random number sequence
in the 8-VSB field sync involves a cross correlation with three ideal PN511 sequences**

# 8 VSB Field Sync PN511 Sequence
recovered from DTV signal

```
0000 0001 0111 .... 1000 0000 1110
```

**Symbol by symbol
Cross-correlation**

```
0000 0001 .... 0000 1110    0000 0001 .... 0000 1110    0000 0001 .... 0000 1110
```

Three PN511 Sequences (Ideal)

Figure A3-2 illustrates the correlation of an ideal 8-VSB signal. A single response is observed at zero microseconds. Otherwise, there is no correlation from −23.69 µs to +23.69 µs (±255 symbols).

FIGURE A3-2

Cross-correlation of an ideal 8-VSB PN511 sequence showing a single main path at zero microseconds
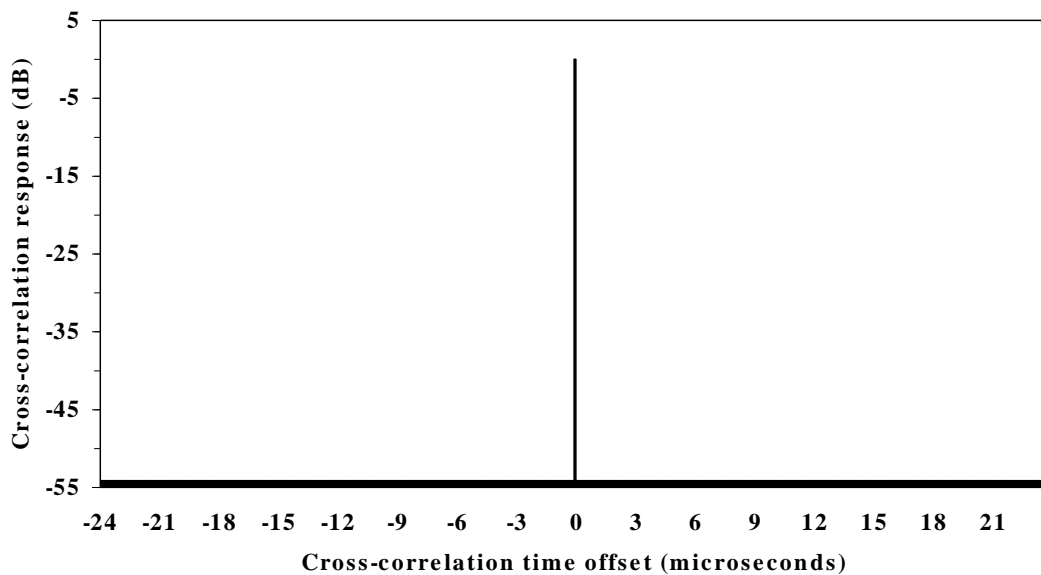
In contrast, Fig. A3-3 shows the channel estimation for a single 10 µs echo captured in the laboratory with a power 6 dB below the main path. In addition to the main path at zero microseconds, the echo is observed at 10 µs. However, the echo appears to have a power lower than the main path by more than 6 dB.

FIGURE A3-3

**Channel estimation of an 8-VSB signal capture in the laboratory
in the presence of a 10 μs echo that is 6 dB lower in power than the main path**
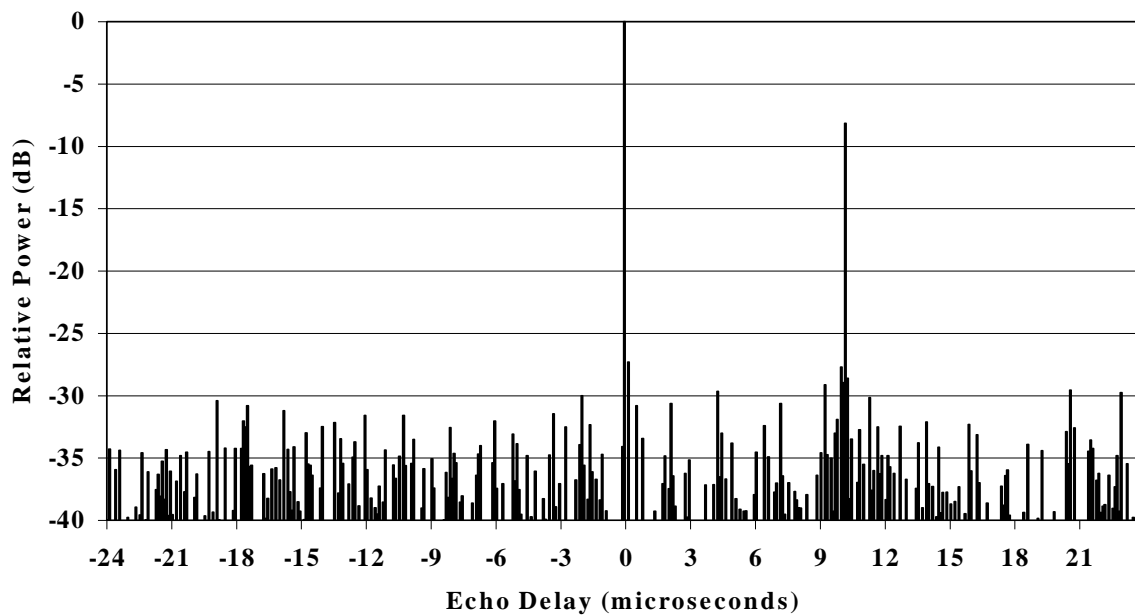
The apparent decrease in echo power is the result of a correlation with only part of the PN511 sequence of the echo. As the delay of the echo moves away from either side of zero, that portion of the echo PN511 sequence included in the correlation diminishes. Consequently, the apparent power in the echo diminishes. In order to obtain the true echo power, the apparent power must be compensated. Figure A3-4 illustrates the compensation factor required to obtain the actual echo power. In the example shown in Fig. A3-3, the 10 μs echo is actually 2 dB higher than the echo power measured by the cross-correlation.

FIGURE A3-4

**Power compensation function required to obtain the actual echo power
from channel estimations using the 8-VSB PN511 sequence**
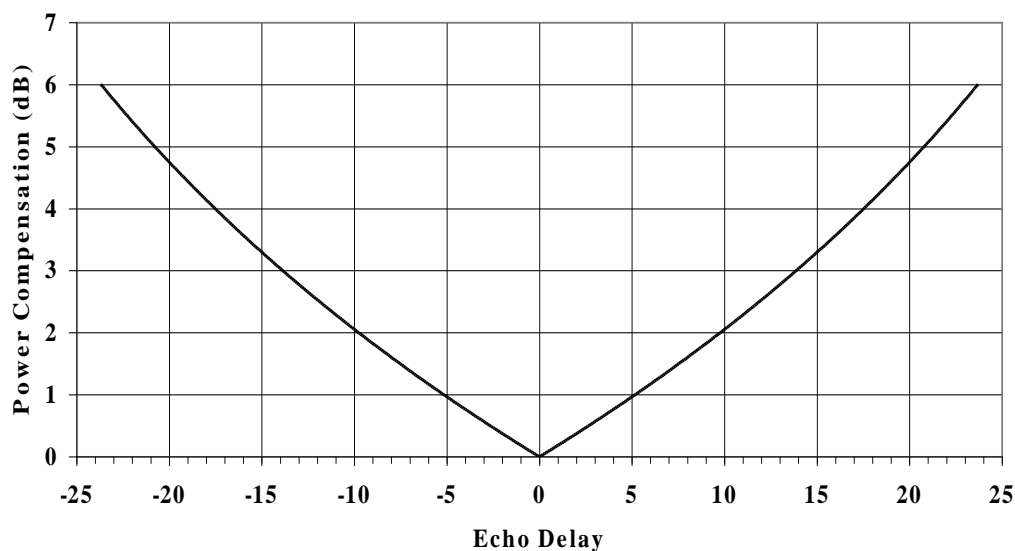
2.2 Channel estimations of Doppler frequency

When one considers evaluating multipath echoes with Doppler in an ATSC receiver (or other digital receiver), it should be remembered that the absolute transmit carrier frequency or phase is unknown because there is no direct carrier reference available in the receiver, as there would be, for example, in a radar system. The radar receiver has the advantage of receiving a direct carrier reference from the transmitter. So, at the radar receiver, it can be discerned which targets (echoes) are moving.

In the case of a DTV receiver, one has no knowledge of the absolute transmit frequency and phase. A relative carrier reference is reconstructed in the receiver that could be the vector sum of the individual multipath components, or perhaps just the dominant path, depending on how carrier recovery is implemented. For example, when it is inferred that a 10 μs post echo has a Doppler rate of say, 3 Hz, the 10 μs echo could, in fact, be perfectly stationary while the dominant path is the one with the Doppler component. One can only speak of "relative" Doppler shifts between the multipath signals and cannot determine for certain the absolute rates of the individual components.

As another example, if a pre-echo is present (not the dominant path signal), it is clear that the dominant path signal is not coming directly from the transmitter site, but is a reflection, as would be any post echo. If the "pre-echo" in such a case were the direct path signal from the transmitter, one would expect it to exhibit very little Doppler (except, perhaps, for tower sway). Consequently the receiver designer should not assume that the dominant signal is stationary in frequency or phase.

2.2.1 Methodology for Doppler Frequency Estimate

Doppler frequencies were computed by observing the amplitude of the real part of the echo from the impulse response of the channel. Since the echo under consideration is isolated (not combined with any other echo), it is similar to observing the real part of a complex phasor over time. The real part of a phasor goes to minimum value at 180 degrees and 360 degrees, and, therefore, has two minimums (or maximums) in a single cycle. By calculating the reciprocal of the time between two minimums of the amplitude of the real part of the echo, the Doppler frequency at which the echo is rotating is obtained. The computation of Doppler frequency has been verified by simulating a synthetic channel with a software modulator and comparing the echo amplitude and Doppler frequency at multiple locations.

3 Analysis of RF captured ATSC signals

This section includes the analysis of nine captured ATSC signals at eight different test sites located in the United States (Washington, DC and New York City) as summarized in Table A3-1 below.

TABLE A3-1

RF signal capture locations

Site	Location	Antenna Location	Antenna height (m)	Antenna type
1	Washington, DC	Outdoor	1.8	Dipole
2	Washington, DC	Indoor	1.2	Double Bowtie
3	Washington, DC	Indoor	1.2	Double Bowtie
4	Washington, DC	Indoor	1.2	Double Bowtie
5	Washington, DC	Outdoor	9.1	Log Periodic
6	Washington, DC	Outdoor	9.1	Log Periodic
7	Washington, DC	Outdoor	9.1	Log Periodic
8 (Loop)	New York, NY	Indoor	1.2	Loop
8 (Bowtie)	New York, NY	Indoor	1.2	Single Bowtie

3.1   Site 1 analysis

Figure A3-5 illustrates the maximum main path power and echo power observed at any given instance within the outdoor signal capture for Site 1. The signal was recorded with a dipole antenna at a height of 1.8 metres in presence of pedestrian traffic. The antenna direction was not optimized for this capture. Although it appears that there is a significant spread in energy around the main path, the multipath conditions remain rather mild, as it was reported that the channel was demodulated by ATSC receivers of different generations.

FIGURE A3-5

Peak echo power as a function of echo delay observed for the duration of the RF capture at Site 1
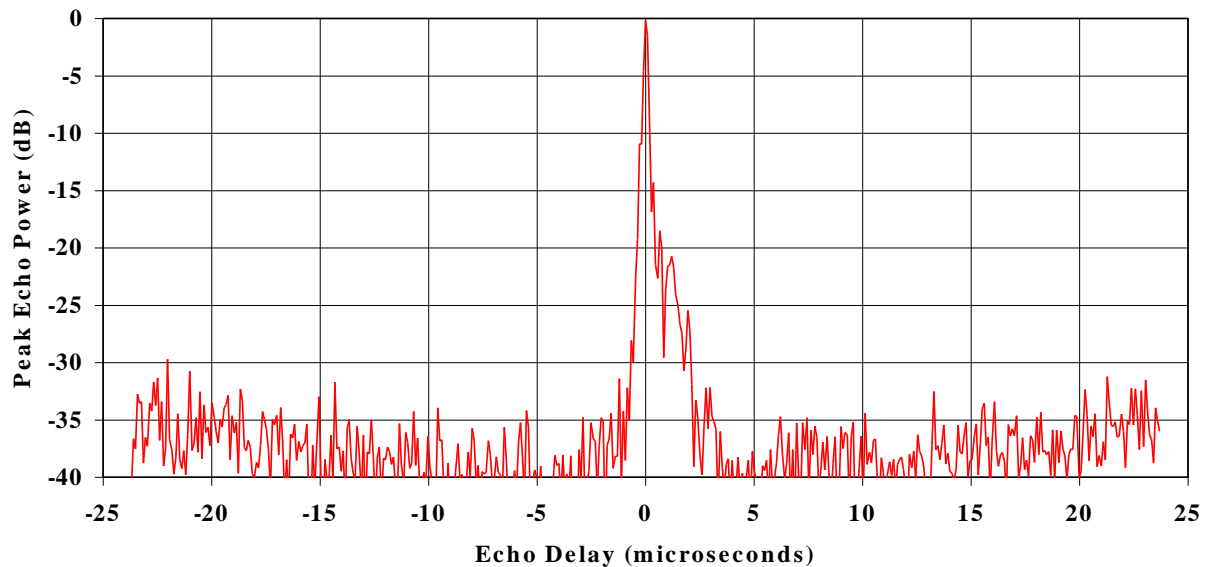
Figure A3-6 illustrates the main power in addition to the echo power for the three greatest "echoes" (+93 ns, −93 ns, and +186 ns) during the RF signal capture at Site 1, showing the dynamic nature around the main path.

FIGURE A3-6

**Power of the main path in addition to the greatest "echoes" shows considerable variation
over the duration of the RF capture for Site 1**
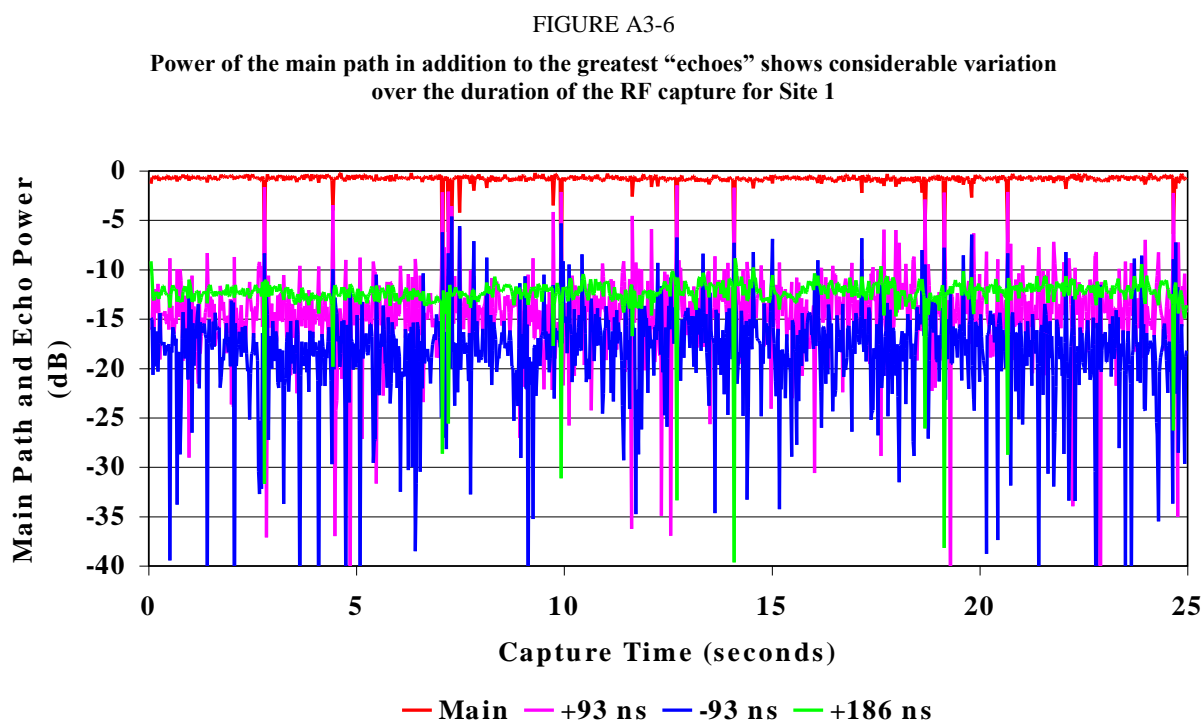
Figure A3-7 demonstrates that it is likely that the main path signal itself is dynamic. This Figure illustrates the total energy of the main path plus six adjacent "echoes" (± 93 ns, ± 186 ns, and ± 279 ns). Note that, even though the main path and the adjacent echoes vary considerably, the total power fluctuation is less than one dB.

FIGURE A3-7

**Total power of the main path and ±3 "echoes" about the main path illustrating
the power is constant even though the main path is dynamic**
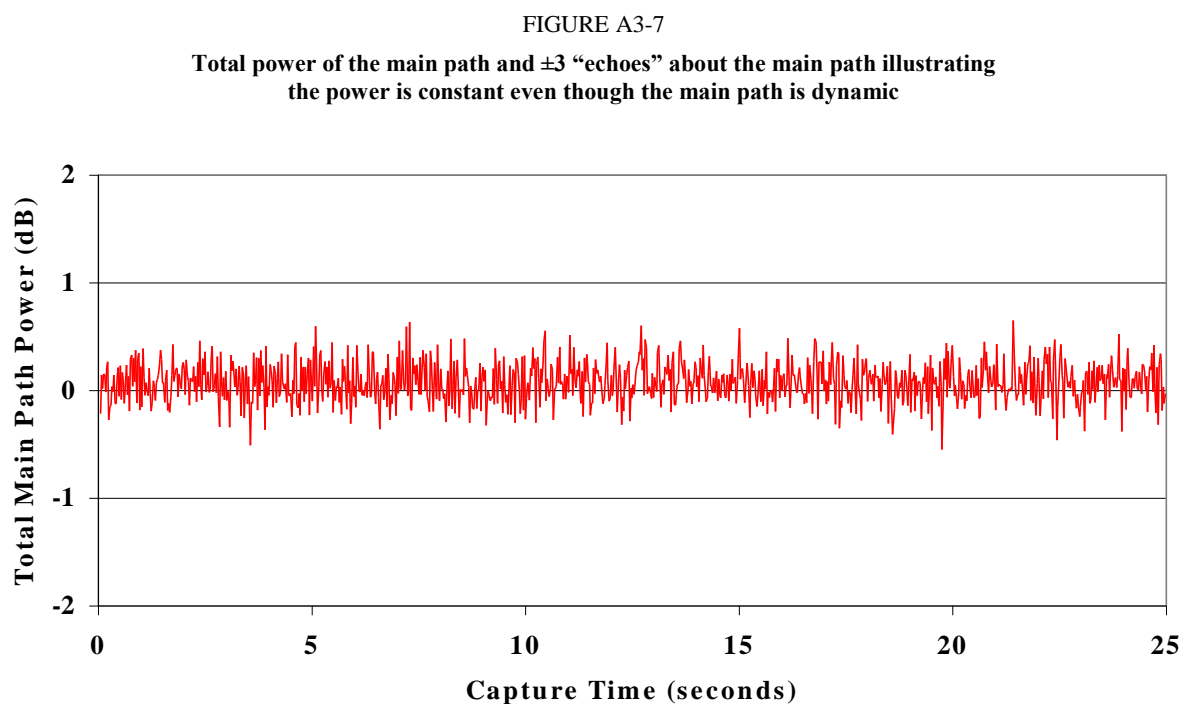
3.2 Site 2 analysis

Figure A3-8 shows the maximum echo powers during the indoor RF signal capture for Site 2. In addition to the spread of energy localized around the main path, the impulse response clearly shows the presence of a post echo around 11 µs with an amplitude relative to the main path of −7 dB maximum.

FIGURE A3-8

Peak echo power as a function of echo delay observed for the duration of the RF capture at indoor Site 2
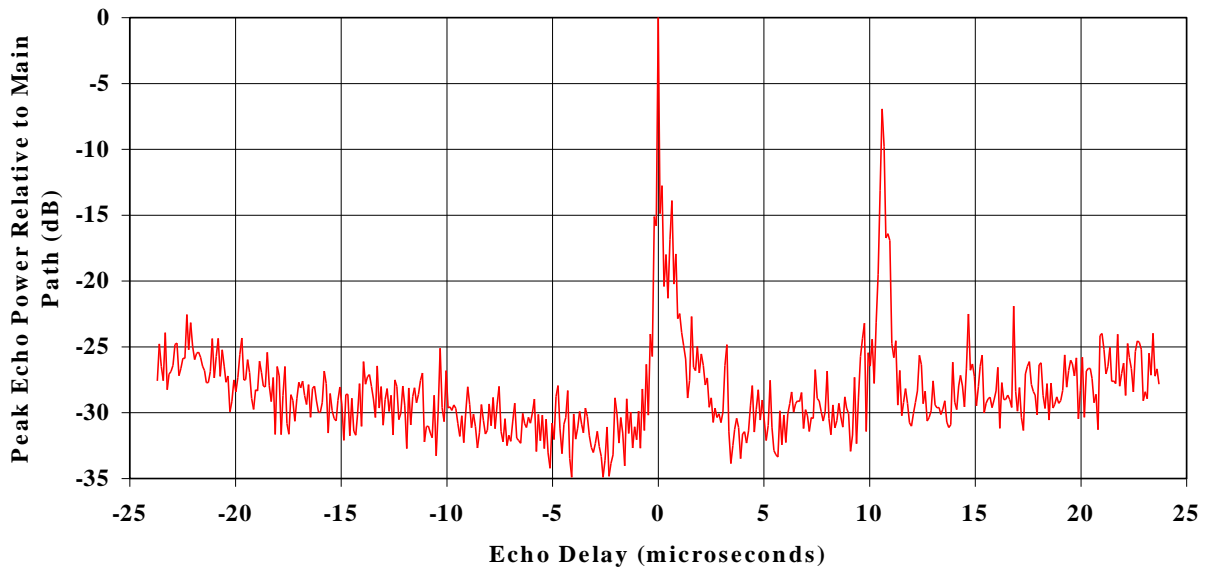
Figure A3-9 shows the magnitude of the post-echo located at +11 μs echo relative to the main path during the start of the capture. This echo is dynamic. The dynamic nature of the echo is interpreted as induced by a Doppler frequency shift with a frequency around 75 Hz (one cycle is completed in approximately 13 ms). For comparison, a line showing the amplitude of the main path is added to the plot.

FIGURE A3-9

**The 11 μs echo magnitude at the beginning of the capture at indoor Site 2
Doppler frequency is 75 Hz**
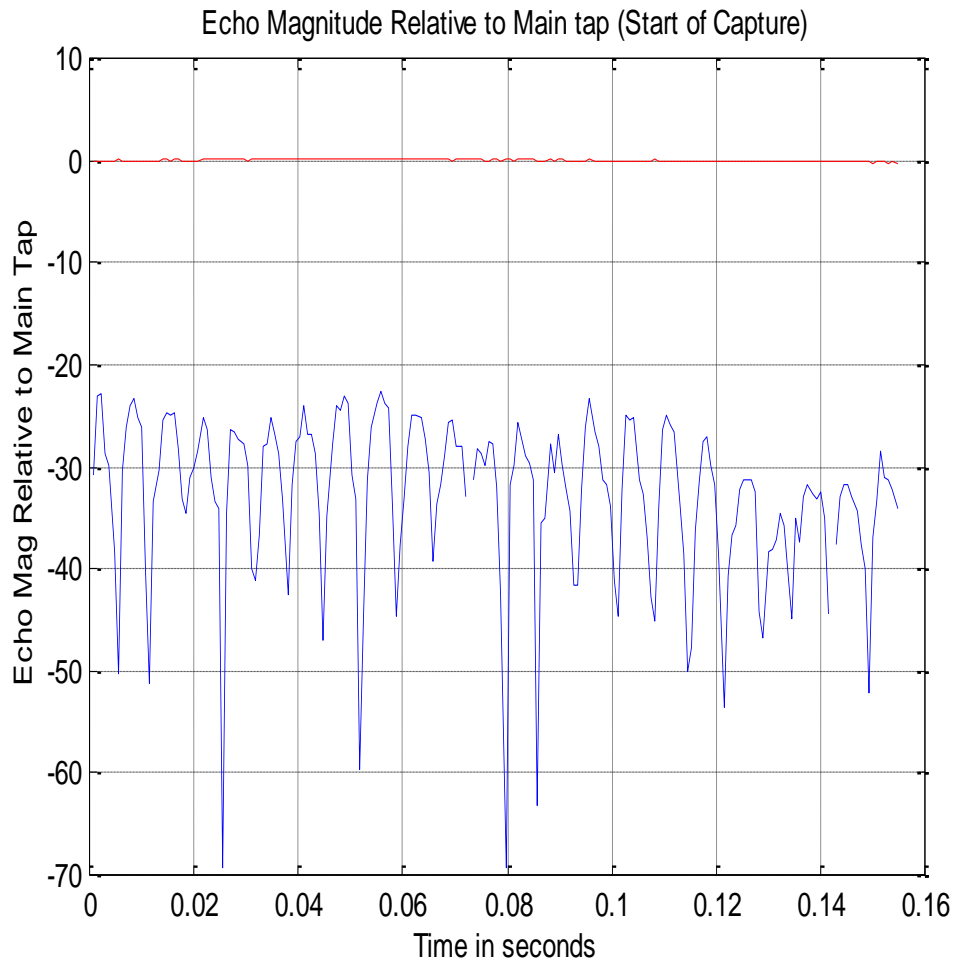
Figure A3-10 shows the magnitude of the 11 μs echo relative to the main path at around 6.7 seconds from the beginning of the capture. We notice that the echo strength is now 15 dB higher than before. The maximum of the echo reaches about −9 dB, which confirms the results furnished in Fig. A3-8. Notice that the Doppler frequency is significantly lower. The cycle time is now around 0.06 seconds, which indicates a Doppler frequency of 17 Hz.

FIGURE A3-10

The 11 μs echo magnitude 6.9 seconds into the capture at indoor Site 2
Doppler frequency is 17 Hz
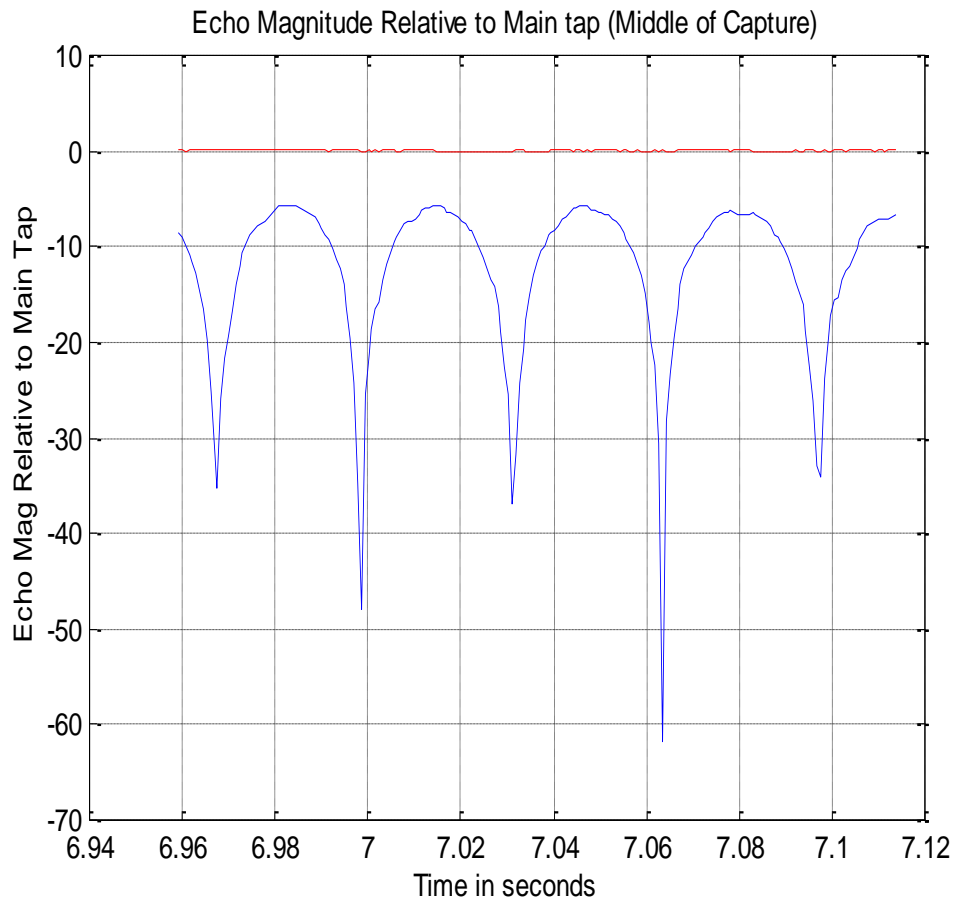
3.3 Site 3 analysis

Figure A3-11 shows the maximum echo power over the entire RF signal capture period. Note that there are equally spaced pre- and post-echoes, as would be expected for the "bobbing channel" (the dominant path swapping between main and post-echo positions). A channel estimate at the beginning of this capture shows that there is a distinct main path and one or more close in echoes. The post echo of principal interest is 1.75 μs from the main path and has a rotating phase, as illustrated in the subsequent Figs A3-12 through A3-18.

FIGURE A3-11

**Peak echo power as a function of echo delay observed for the duration of the RF capture at indoor Site 3
The evenly spaced echoes peaked at ±1.67 μs indicate that the main path and the echo alternate
— a "bobbing" channel**
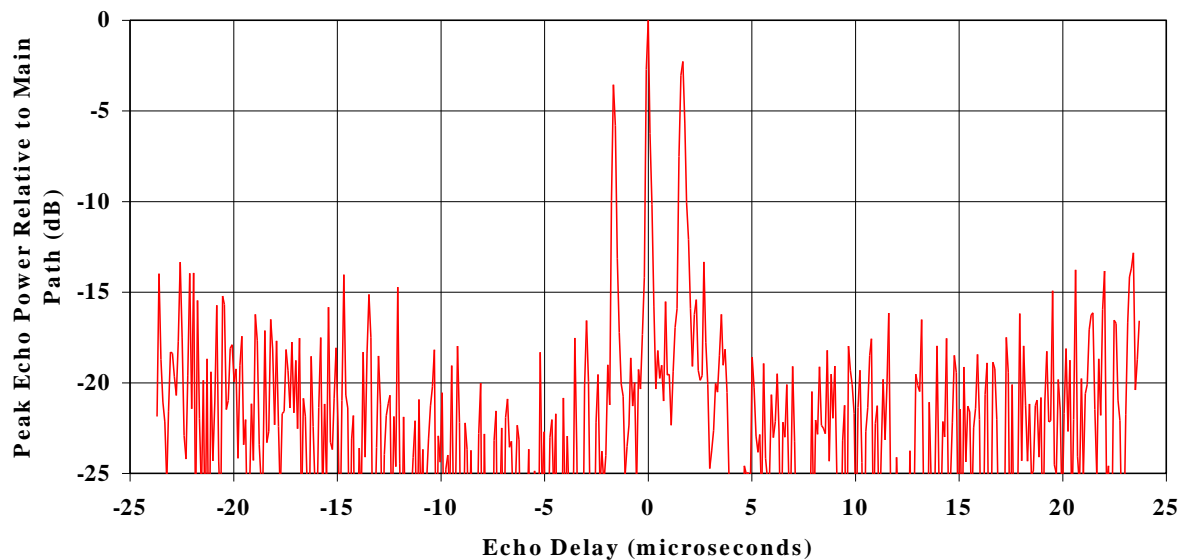
Figure A3-12 shows the magnitude of the 1.75 µs echo relative to the main path over a period of about 0.16 seconds at the beginning of the capture. Notice that the main path amplitude is constant, whereas the echo has variable amplitude. The cycle time for this echo at this time is around 25 ms, which gives a Doppler frequency of about 40 Hz. The echo magnitude is around −15 dB relative to the main path.

FIGURE A3-12

Echo magnitude for the 1.75 µs echo relative to the main path at the beginning of the capture at indoor Site 3. The echo magnitude is −15 dB relative to the main path. The Doppler frequency is 40 Hz
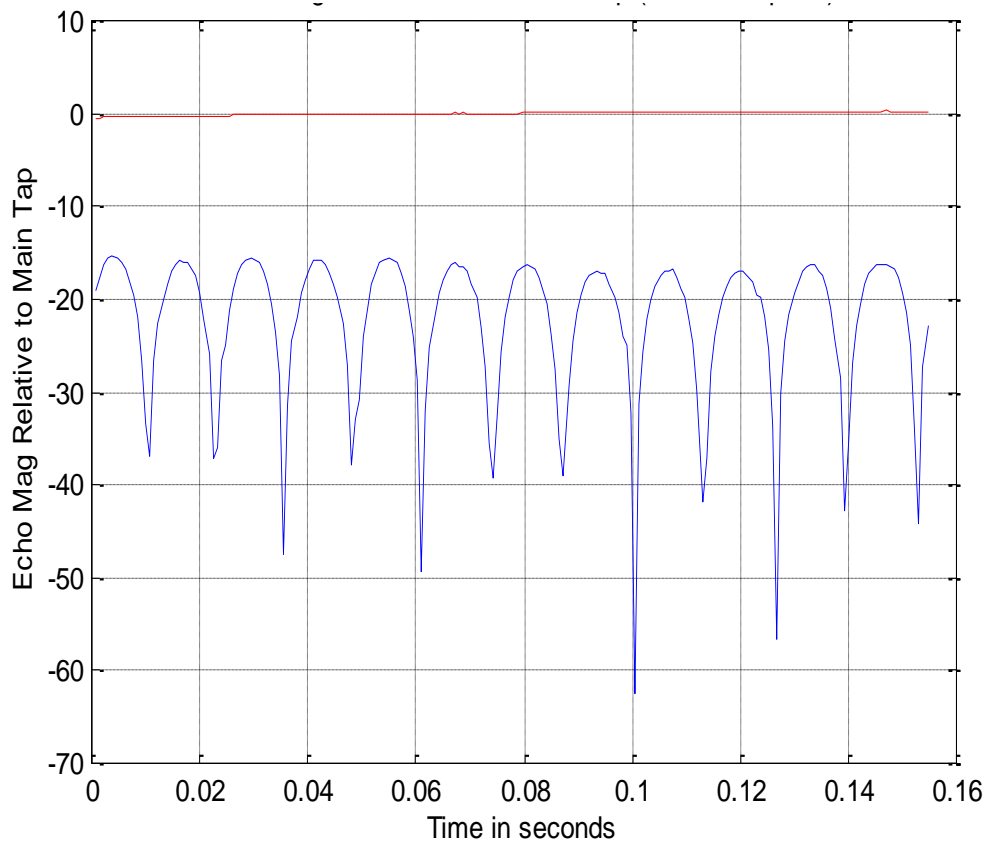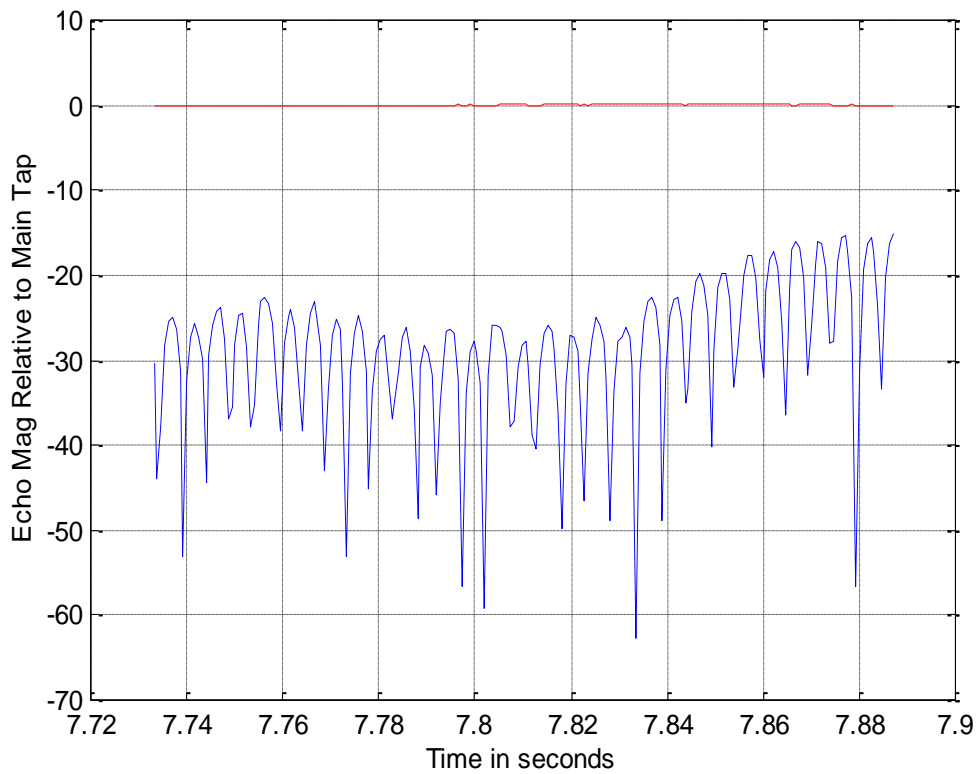

Figure A3-13 shows the magnitude of the 1.75 µs echo relative to the main path, 3 seconds into the capture. Notice that the main path amplitude is constant, whereas the echo has variable amplitude due to the Doppler phase rotation. The cycle time for this echo at this time is around 59 ms, which gives a Doppler frequency of about 17 Hz. The echo magnitude is about −5 dB relative to the main path.

FIGURE A3-13

**Echo magnitude for the 1.75 μs echo relative to the main path, 3 seconds into the capture at indoor Site 3.
The echo magnitude is –5 dB relative to the main path and has a Doppler frequency of 17 Hz**
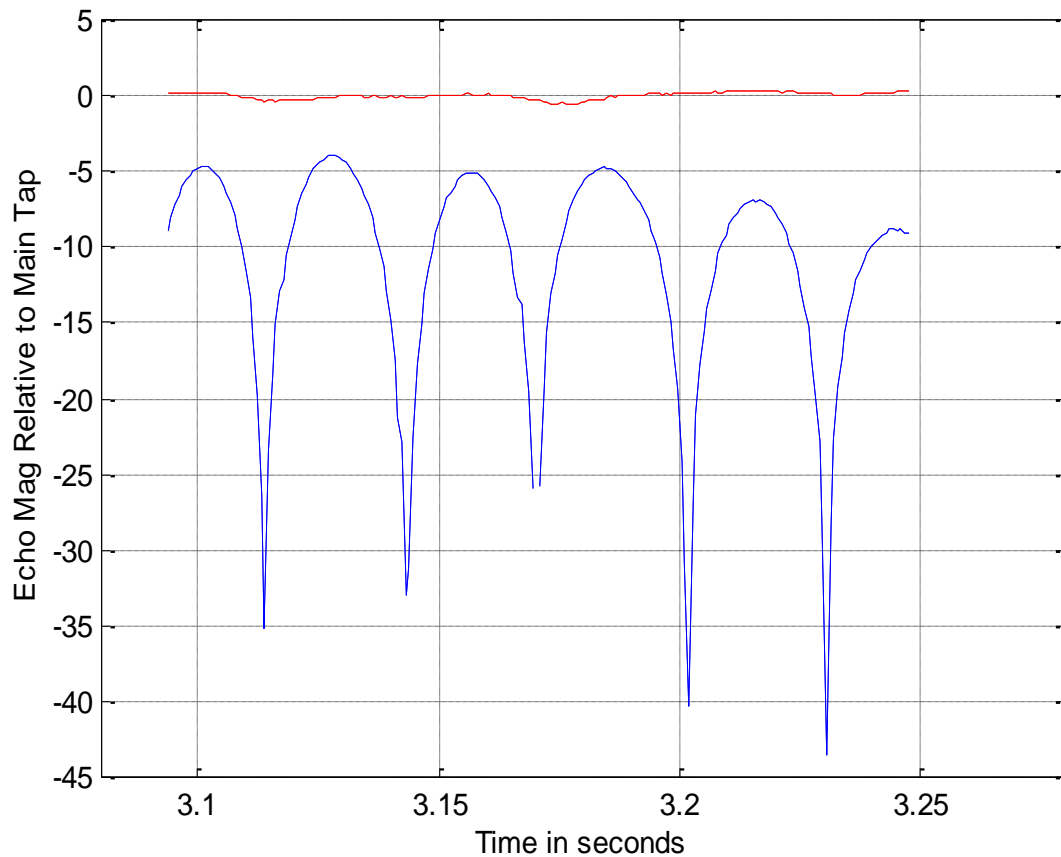
Figure A3-14 shows the magnitude of the 1.75 μs echo relative to the main path, 7.5 seconds into the capture. Notice that the main path amplitude is constant, whereas the echo has variable amplitude due to the Doppler phase rotation. The cycle time for this echo, at this time, is around 11.5 ms, which gives a Doppler frequency of about 80 Hz. The echo magnitude is about –25 dB to –15 dB relative to the main path.

FIGURE A3-14

Echo magnitude for the 1.75 μs echo relative to the main path, 7.5 seconds into the capture at indoor Site 3. The echo magnitude is –25 dB to –15 dB relative to the main path and has a Doppler frequency of 80 Hz

Figure A3-15 shows the magnitude of the 1.75 μs echo relative to the main path, 9.2 seconds into the capture. Notice that the main path amplitude is constant, whereas the echo has variable amplitude due to the Doppler phase rotation. The cycle time for this echo, at this time, is around 6.5 ms, which gives a Doppler frequency of about 150 Hz. The echo magnitude is about –25 dB to –20 dB relative to the main path.

FIGURE A3-15

Echo magnitude for the 1.75 µs echo relative to the main path, 9.2 seconds into the capture at indoor Site 3.
The echo magnitude is –25 dB to –20 dB relative to the main path and has a Doppler frequency of 150 Hz
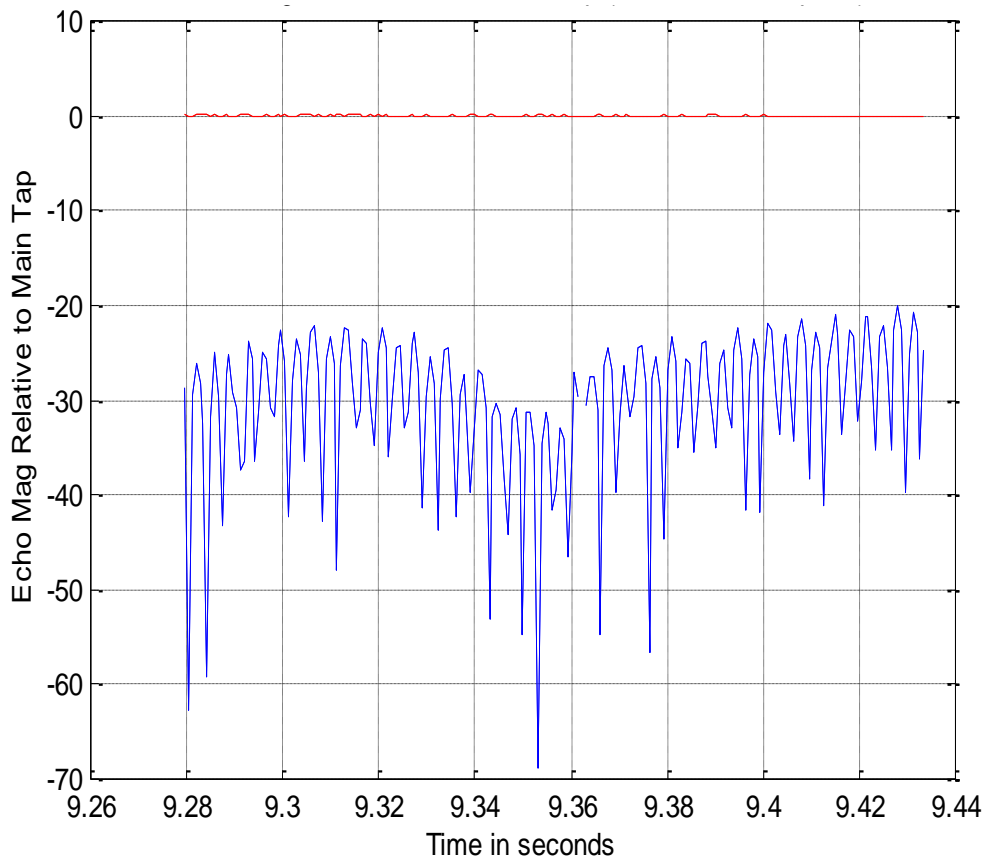
Taking another intermediate look at the RF capture for Site 3, a "bobbing" channel appears. Figures A3-16, A3-17, and A3-18, occurring at 5.167, 5.227, and 5.279 seconds into the capture, respectively, depict the main path and the post-echo exchanging positions. This confirms the two peaks shown in Figure A3-11.

FIGURE A3-16

**Channel estimate (absolute value) for the RF capture at indoor Site 3 at 5.167 seconds
into the capture, showing the main path and a 1.75 μs echo**
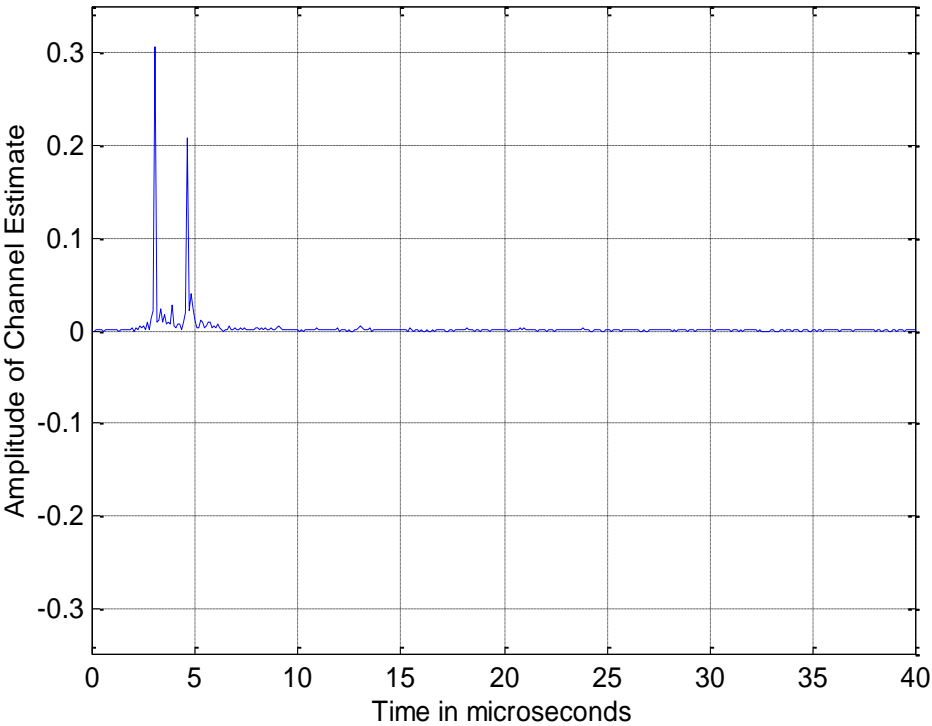
FIGURE A3-17

**Channel estimate (absolute value) for the RF capture at indoor Site 3 at 5.279 seconds, showing the main path and a 1.75 μs
echo. The 1.75 μs echo has increased in magnitude with respect to the main path**
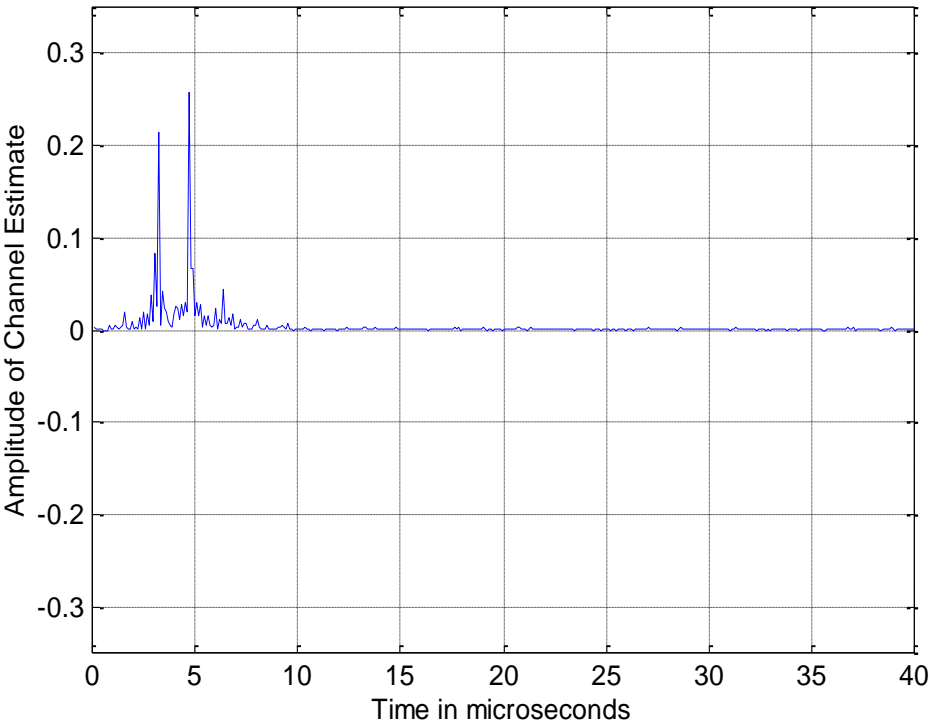
FIGURE A3-18

Channel estimate (absolute value) for the RF capture at indoor Site 3 at 5.279 seconds, showing the main path and a 1.75 μs echo. The 1.75 μs echo is now a post echo with respect to the main path
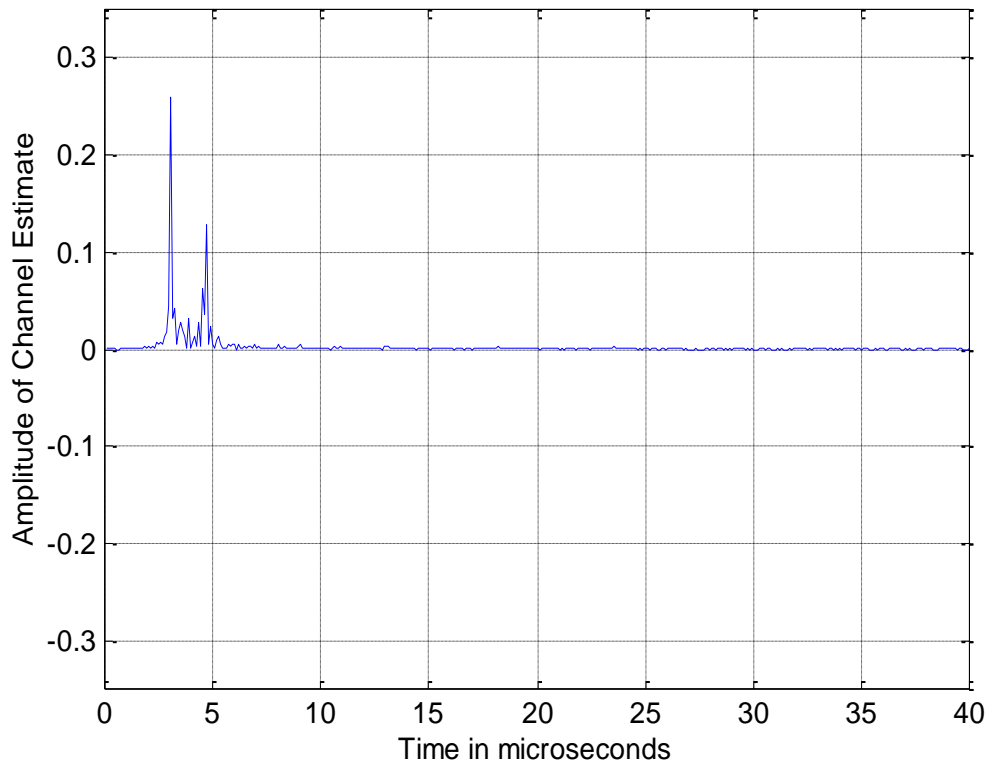
3.4 Site 4 analysis

Figure A3-19 illustrates the peak echo power relative to the main power throughout a 25 second RF capture for the indoor Site 4. The capture has a dynamic main path as well as strong dynamic pre-echoes at −1.95 μs and −3.07 μs and a post-echo at +15.6 μs. Site 4 is a "town house" located 15.4 km from the transmitter.

FIGURE A3-19

Peak echo power as a function of echo delay observed for the duration of the RF capture at indoor Site 4
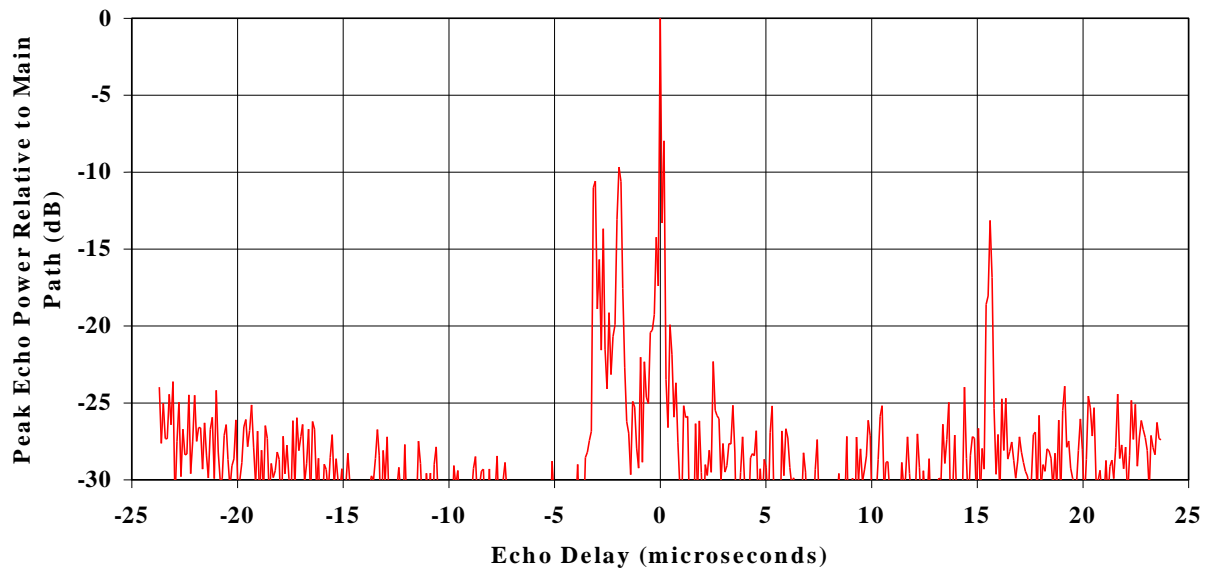
It is instructive to note that the DTV channel illustrated in Fig. A3-19 has echoes prior to the main or dominate path (pre-echo). A different DTV channel at the same Site 4 exhibited the pre-echo as the main path and the main path in Fig. A3-19 as a post-echo. That is, the echo and the main path have exchanged positions. The echo amplitudes are relatively constant over time in each capture, however, and can therefore be characterized as static. Both channels have a weak echo at 18.5 μs.

Figure A3-20 illustrates the echo power for Site 4 over the entire 25-second capture. Notice the presence of a slow Doppler affecting the three principal echoes.
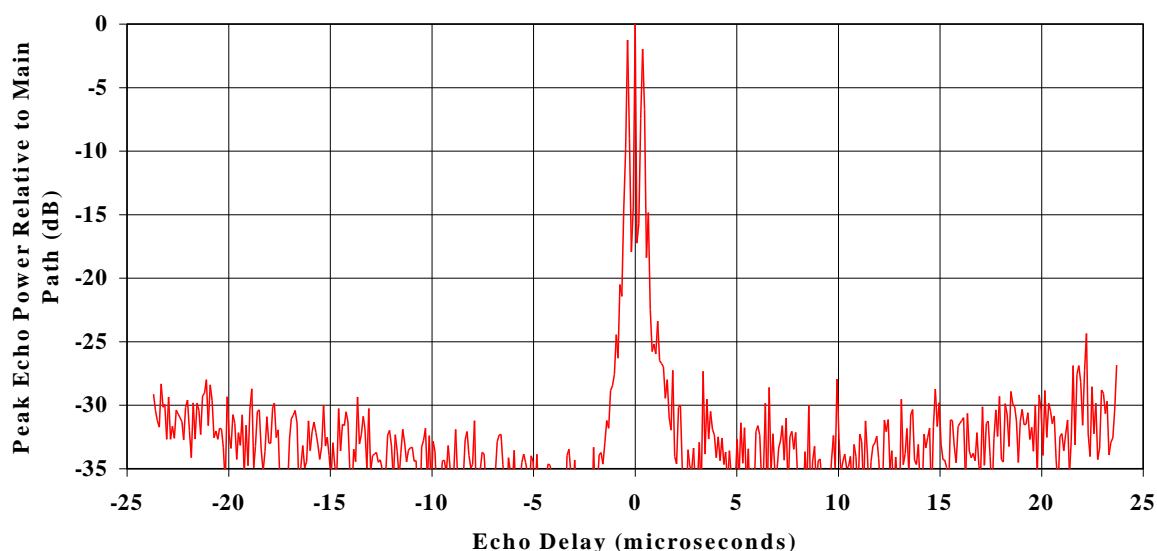
FIGURE A3-20

Power of the main path and three main echoes illustrates the dynamic nature of echoes for indoor Site 4
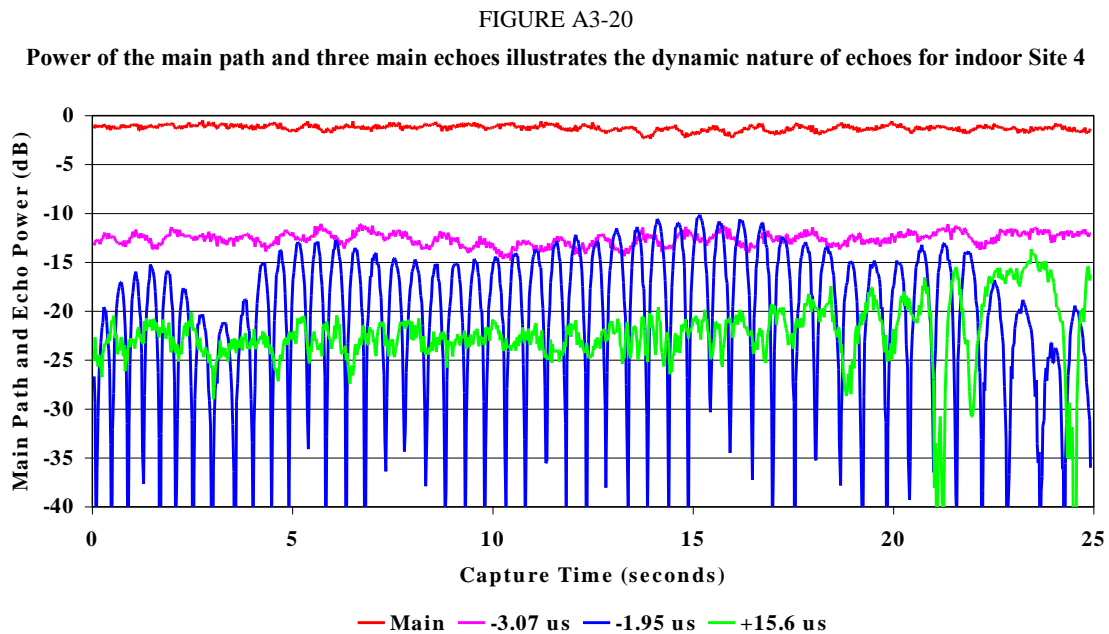
3.5 Site 5 analysis

Another example of a "bobbing" channel is provided with the outdoor RF capture at Site 5. This outdoor field capture involved no direct transmission path, even though the receive antenna was only 6.3 km from the transmit antenna. Figure A3-21 illustrates the maximum main path power and echo power observed at any given instance within the capture. The evenly spaced, close-in echoes, peaked at ±372 ns, indicate that the "main" and "echo" paths alternate.

FIGURE A3-21

**Peak echo power as a function of echo delay observed for the duration of the RF capture at outdoor Site 5.
The evenly spaced close-in echoes peaked at ±372 ns indicate that the main path and the echo alternate
— a "bobbing" channel**

The "bobbing" nature of the echoes is evident in Figs A3-22 and A3-23. At 22.906 seconds into the capture, a strong 372 ns pre-echo is present, as illustrated in Figure A3-22.
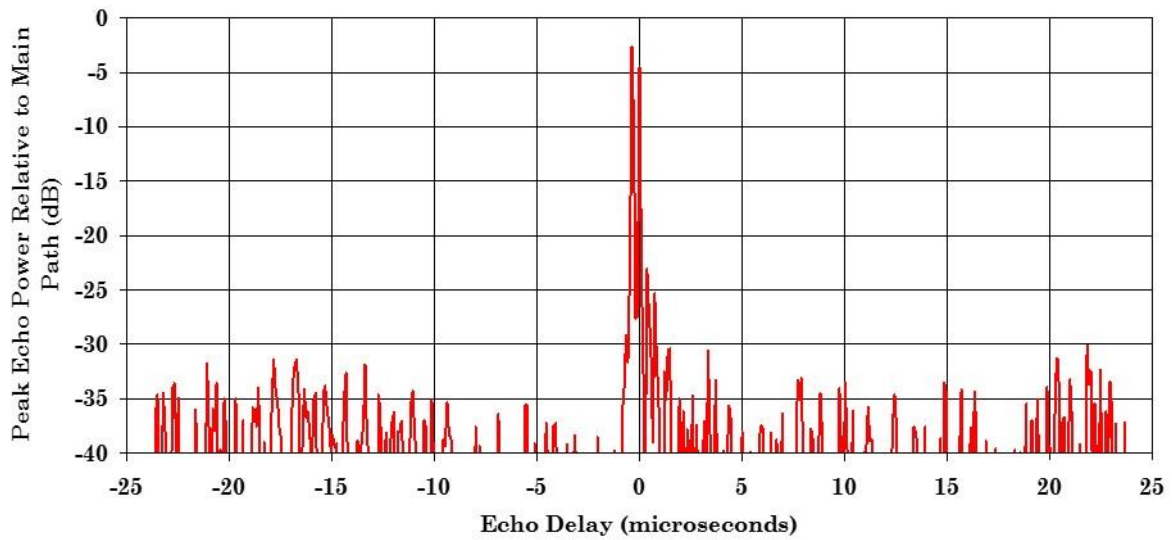
FIGURE A3-22

**Echo power as a function of echo delay observed at 22.906 seconds into the RF capture of outdoor Site 5.
A strong pre-echo is present at −372 ns**
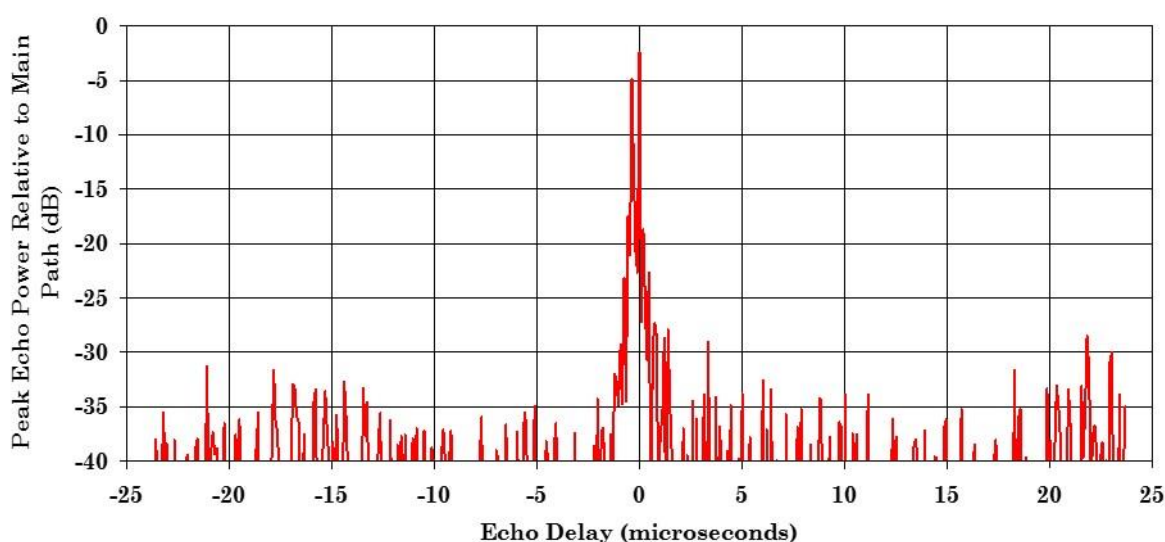
Two field syncs later in time (at 22.955 seconds), the formerly pre-echo path now exceeds the main path, as illustrated in Fig. A3-23. The original echo has become the dominant path. It is clear that signal conditions do exist where, although the receive antenna is directional and 9.1 metres high, strong echoes can be present and may even exceed the dominant path in signal level.

FIGURE A3-23

**Echo power as a function of echo delay observed at 22.955 seconds into the RF capture of outdoor Site 5.
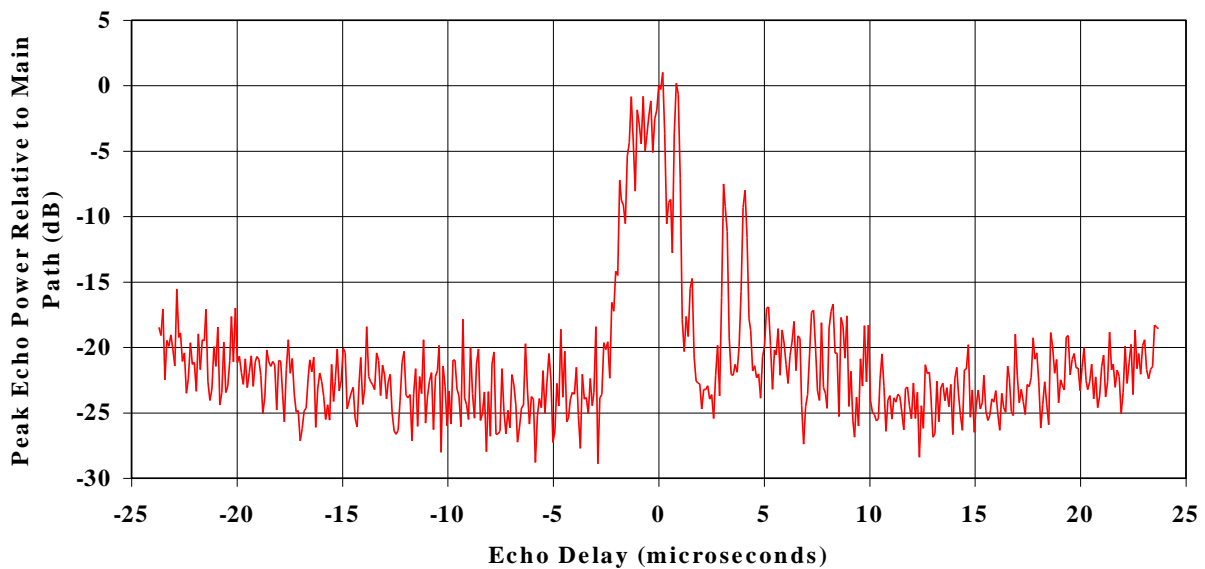After two additional field syncs in time, the 372 ns pre-echo is now the dominant path**

3.6   Site 6 analysis

Figure A3-24 illustrates the peak echo power of the RF outdoor capture at Site 6. The Figure demonstrates the presence of strong pre- and post-echoes that are close in delay to the main path.

FIGURE A3-24

Peak echo power observed in RF capture at Site 6

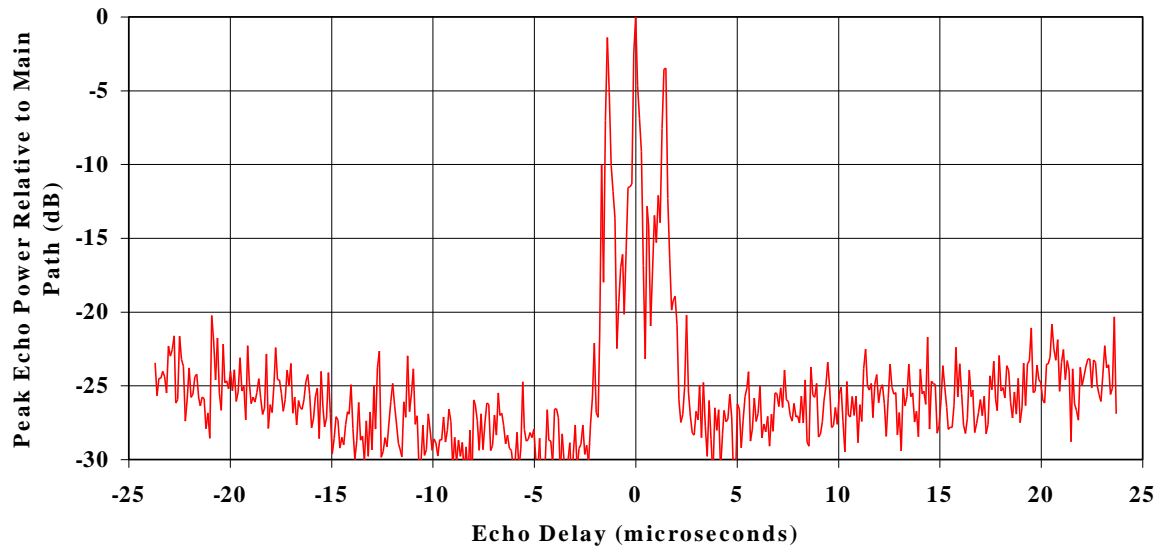

3.7   Site 7 analysis

Figure A3-25 illustrates the peak echo power of the RF outdoor capture at Site 7. This channel has a pattern characteristic of a close-in "bobbing channel".
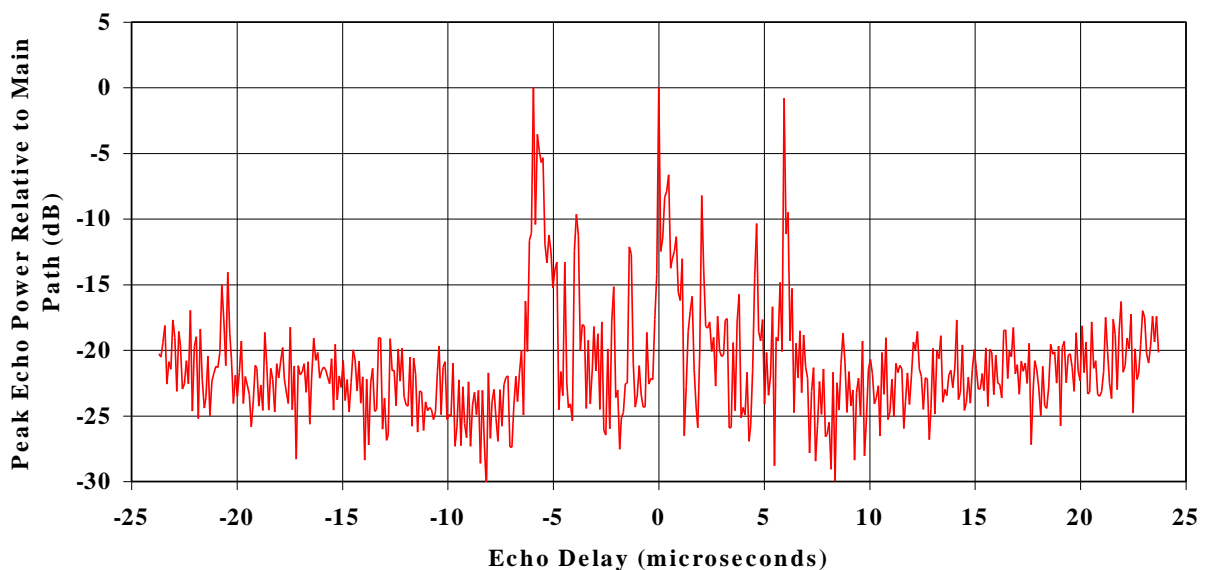
FIGURE A3-25

Peak echo power observed in RF capture at Site 7

3.8 Site 8 (Loop) analysis

Figure A3-26 shows the peak echo power for indoor reception at Site 8 captured with a loop-type antenna, 1.8 metres above floor level. The Figure demonstrates the presence of both strong pre and post-echoes. The capture location was a fourth-floor urban apartment constructed of wood with brick siding. The room had windows on two adjacent walls.
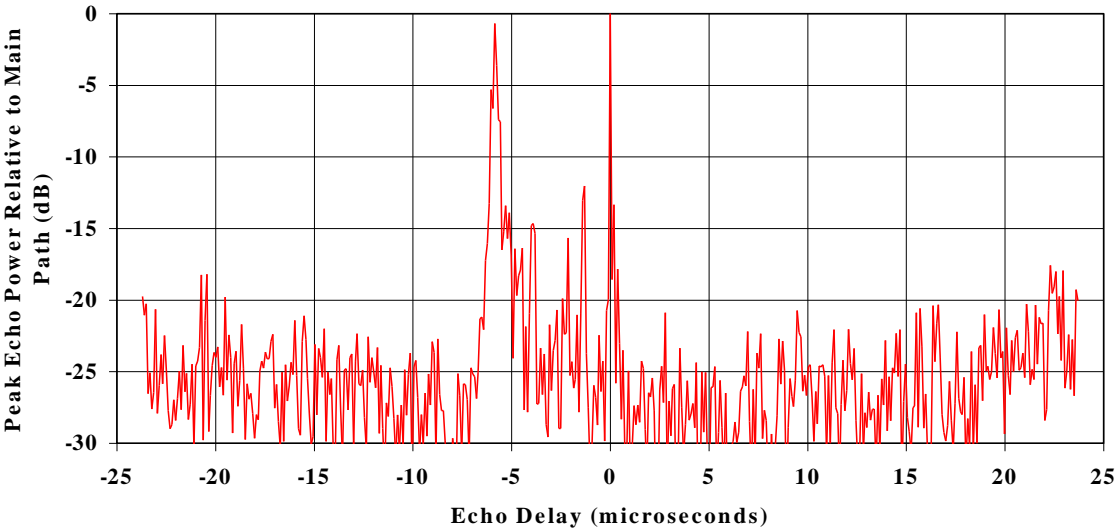
FIGURE A3-26

**Peak echo power observed in RF capture at Site 8
using a loop-type antenna in a fourth-floor urban apartment**

3.9 Site 8 (Bowtie) analysis

Figure A3-27 shows the peak echo power for indoor reception at Site 8 captured at the same location as section 3.8 above, using a single bowtie-type antenna at 1.8 metres above floor level.

FIGURE A3-27

**Peak echo power observed in the RF capture at Site 8
using a single bowtie-type antenna in a fourth-floor urban apartment**

_____